

Observational constraints on cosmic neutrinos and dark energy revisited

Xin Wang,^{a,b} Xiao-Lei Meng,^{a,c} Tong-Jie Zhang,^{a,d} HuanYuan Shan,^{e,f}
Yan Gong,^g Charling Tao,^{e,f} Xuelei Chen,^c Y. F. Huang^b

^aDepartment of Astronomy, Beijing Normal University, Beijing 100875, China

^bSchool of Astronomy and Space Science, Nanjing University, Nanjing, 210093, China

^cNational Astronomical Observatories, Chinese Academy of Sciences, Beijing 100012, China

^dKavli Institute for Theoretical Physics China, CAS, Beijing 100190, China

^eDepartment of Physics and Tsinghua Center for Astrophysics, Tsinghua University, Beijing, 100084, China

^fCentre de Physique des Particules de Marseille, CNRS/IN2P3-Luminy and Université de la Méditerranée, Case 907, F-13288 Marseille Cedex 9, France

^gDepartment of Physics and Astronomy, University of California, Irvine, CA 92697

E-mail: tjzhang@bnu.edu.cn

Abstract. Using several cosmological observations, i.e. the cosmic microwave background anisotropies (WMAP), the weak gravitational lensing (CFHTLS), the measurements of baryon acoustic oscillations (SDSS+WiggleZ), the most recent observational Hubble parameter data, the Union2.1 compilation of type Ia supernovae, and the HST prior, we impose constraints on the sum of neutrino masses ($\sum m_\nu$), the effective number of neutrino species (N_{eff}) and dark energy equation of state (w), individually and collectively. We find that a tight upper limit on $\sum m_\nu$ can be extracted from the full data combination, if N_{eff} and w are fixed. However this upper bound is severely weakened if N_{eff} and w are allowed to vary. This result naturally raises questions on the robustness of previous strict upper bounds on $\sum m_\nu$, ever reported in the literature. The best-fit values from our most generalized constraint read $\sum m_\nu = 0.556^{+0.231}_{-0.288}$ eV, $N_{\text{eff}} = 3.839 \pm 0.452$, and $w = -1.058 \pm 0.088$ at 68% confidence level, which shows a firm lower limit on total neutrino mass, favors an extra light degree of freedom, and supports the cosmological constant model. The current weak lensing data are already helpful in constraining cosmological model parameters for fixed w . The dataset of Hubble parameter gains numerous advantages over supernovae when $w = -1$, particularly its illuminating power in constraining N_{eff} . As long as w is included as a free parameter, it is still the standardizable candles of type Ia supernovae that play the most dominant role in the parameter constraints.

Keywords: neutrino properties — neutrino masses from cosmology — weak gravitational lensing — power spectrum

Contents

1	Introduction	1
2	Observables and Data	3
2.1	Weak Gravitational Lensing	4
2.2	Type Ia Supernovae	5
2.3	Baryon Acoustic Oscillations	6
2.4	Observational Hubble Parameter Data	6
2.5	Further Data and Priors	6
3	Constraints on Cosmological Parameters	7
3.1	Vanilla+ $\sum m_\nu$	7
3.2	Vanilla+ N_{eff}	8
3.3	Vanilla+ $\sum m_\nu+N_{\text{eff}}$	9
3.4	Vanilla+w+ $\sum m_\nu$	9
3.5	Vanilla+w+ N_{eff}	10
3.6	Vanilla+w+ $\sum m_\nu+N_{\text{eff}}$	10
4	Neutrino Impact on Structure Formation	11
5	Conclusion and Discussion	13

1 Introduction

One of the most intriguing mysteries in modern cosmology is the property of cosmic neutrinos. Directly from the oscillation experiments [1], it is known that

$$\begin{aligned}\Delta m_{\text{atm}}^2 &= |\Delta m_{31}^2| = (2.2_{-0.5}^{+0.7}) \times 10^{-3} \text{eV}^2 \\ \Delta m_{\text{sun}}^2 &= \Delta m_{21}^2 = (8.1_{-0.6}^{+0.6}) \times 10^{-5} \text{eV}^2,\end{aligned}\tag{1.1}$$

where $\Delta m_{ij}^2 = m_i^2 - m_j^2$ is the squared mass difference between two neutrino eigenstates. This result naturally leads to three scenarios for the mass splitting of the standard three flavor neutrinos [2]:

- (I) Normal Hierarchy — $m_1 \sim 0$, $m_2 \sim \Delta m_{\text{sun}}$, and $m_3 \sim \Delta m_{\text{atm}}$;
- (II) Inverted Hierarchy — $m_1 \sim m_2 \sim \Delta m_{\text{atm}}$, and $m_3 \sim 0$;
- (III) Total Degeneracy — $m_1 \sim m_2 \sim m_3 \gg \Delta m_{\text{atm}}$.

Although the absolute values of neutrino masses are beyond the reach of oscillation experiments, other ground-based experiments, e.g. measurements of tritium beta decay [3] and neutrinoless double beta decay [4], provide some hints on the overall mass scale. Nevertheless, the most compelling bounds on the total mass of neutrinos ($\sum m_\nu$) come from the cosmos (for recent reviews, see Refs. [5, 6]). Firstly, the anisotropies of the cosmic microwave background (CMB) are sensitive to neutrino masses [7]. As massive neutrinos become non-relativistic, their contributions to the energy constituent changes from radiation-like to matter-like. Provided that these neutrinos are massive enough, they will slow down to non-relativistic speed even before the recombination epoch. This slight modification in expansion history affects acoustic peaks. Small scale anisotropies are meanwhile boosted, due to the enhancement of photon energy density fluctuations by the diminishing

gravitational potentials [8]. The latest observations of WMAP seven-year pin down the 95% upper limit of $\sum m_\nu$ to 1.3 eV [9], while Planck and other next-term probes are presumably capable of pushing forward the sensitivity to $\sum m_\nu \sim 0.2 - 0.03$ eV, [10–12]. Secondly, massive neutrinos affect the evolution of matter perturbation in a particular way: they erase the density contrast at wavelengths smaller than their characteristic free-streaming scale, resulting in a suppression of linear matter power spectrum as given by [13],

$$\frac{\Delta P_{\text{lin}}(k)}{P_{\text{lin}}(k)} \sim -8 \frac{\Omega_\nu}{\Omega_m}. \quad (1.2)$$

with $\Omega_\nu = \sum m_\nu / (93.8 h^2 \text{ eV})$ being the neutrino matter density fraction [2]. Thus the constraint on the sum of neutrino masses greatly benefits from accurate measurements of matter power spectrum. A great deal of effort has been dedicated to reducing the upper limit of $\sum m_\nu$ from a number of large scale structure projects, e.g. 2dFGRS, SDSS, WiggleZ, CFHTLS galaxy surveys [14–32]. The present record gives $\sum m_\nu < 0.26$ eV at 95% confidence level (CL), using the combination of WMAP seven-year data, SDSS DR8 LRG angular spectra together with the HST prior [33].

Another novel and independent tracer of matter clustering is weak gravitational lensing (WL), i.e. the bending of light through intervening inhomogeneous mass distribution, which as a result generates small distortion (at the 1% level) on the images of distant sources. Since the first detection of cosmic shear [34–37], WL has been repeatedly shown to be a powerful and precise approach to measure mass fluctuations and constrain cosmological models (see Ref. [38] for a thorough review). The greatest advantage of WL is that it only relies on the total matter content along the line of sight, and is therefore free from the problematic modeling of galaxy-to-matter bias [39]. Using Fisher formalism, several studies have forecasted the error budget of future WL surveys constraining neutrino masses [40–43]. However, there are few groups who have put actual constraints on $\sum m_\nu$ from current observational results [44]. In particular, using up-to-date WL data of CFHTLS-T0003 and other cosmological probes, Ref. [45] and Ref. [46] obtained the mutually consistent result, an 95% upper bound of $\sum m_\nu < 0.54$ eV.

Known as cosmic chronometers, the observational Hubble parameter data (OHD) have recently gained increasing attention in their potential of measuring the geometry and matter content of the universe [47, 48]. The Hubble expansion rates at different redshifts can be obtained via the differential-age technique [49, 50]. Compared with the type Ia supernovae (SNIa) data, OHD have the virtue of being directly linked to the expansion history, whereas what SNIa measure is luminosity distance, related to $H(z)$ through integration. Using the latest OHD data, Ref. [51] has derived competitive upper limits on the total neutrino mass, $\sum m_\nu < 0.24$ eV at 68% CL.

Although there has been a vast scope of work on the constraints on $\sum m_\nu$ previously, most of these analyses do not seek appropriate treatments of correlations associated with $\sum m_\nu$ and other cosmological parameters. As argued by Ref. [52], the degeneracy between $\sum m_\nu$ and the dark energy equation of state (EOS) parameter w fatally weakens the constraints on $\sum m_\nu$. Except the role of dark energy, the effective number of neutrino species, i.e. N_{eff} , remarkably lifts the bounds on $\sum m_\nu$, attributed to their correlation [53–55]. Standard primordial nucleosynthesis with weak interaction rate corrections yields $N_{\text{eff}} = 3.046$ [56]. Here this non-integer part originates from the non-thermal feature in neutrino distribution function due to partial heating during e^\pm annihilations, including both finite temperature QED corrections and flavor oscillation effects [57–59]. However, as proven more and more firmly by the series of WMAP papers, N_{eff} seems to be much larger than the standard value [9, 60, 61]. Similar conclusions are also reached by other small scale CMB observations, e.g. $N_{\text{eff}} = 4.6 \pm 0.8$ for ACT, and $N_{\text{eff}} = 3.86 \pm 0.42$ for SPT [62, 63]. The presence of extra light degrees of freedom, called “dark radiation”, might be reasonably explained by some light sterile neutrinos, axions or majorons in thermal equilibrium after the QCD phase transition [64–66]. As a consequence,

most of the upper limits on $\sum m_\nu$, which are derived fixing $N_{\text{eff}} = 3.046$, seem too optimistic. We note that recently Ref. [67] uses several updated cosmological probes to deliver one of the most comprehensive investigations on the $(\sum m_\nu, N_{\text{eff}}, w)$ constraints and their correlations. However Ref. [67] does not focus on comparing different sets of cosmological data, and furthermore it does not use one of the most promising techniques, i.e. WL. In this work, we would like to concentrate on the correlations between some key parameters including $(\sum m_\nu, N_{\text{eff}}, w)$, and also investigate how their individual values and degeneracies affect the constraints as well as dark matter clustering. Particularly, we will study the role of WL, and compare the constraining ability of SNIa and OHD.

The outline of our paper is as follows. Sect. 2 introduces the observational data in our analysis. Then we present the main constraint results in Sect. 3. In Sect. 4 we investigate in detail the impacts of the three key parameters $(\sum m_\nu, N_{\text{eff}}, w)$ on structure formation. Finally Sect. 5 presents our conclusion and discussion.

2 Observables and Data

In this section, we briefly introduce the cosmological probes selected for neutrino constraints. In the context of Friedmann-Robertson-Walker metric, it is simple to derive the coordinate distance r in terms of the radial distance χ as [68]

$$r(\chi) = \begin{cases} \frac{c}{H_0 \sqrt{\Omega_k}} \sinh\left(\frac{H_0 \sqrt{\Omega_k}}{c} \chi\right) & \text{if } \Omega_k > 0, \\ \chi & \text{if } \Omega_k = 0, \\ \frac{c}{H_0 \sqrt{|\Omega_k|}} \sin\left(\frac{H_0 \sqrt{|\Omega_k|}}{c} \chi\right) & \text{if } \Omega_k < 0, \end{cases} \quad (2.1)$$

with χ and r also known as the comoving distance and the comoving angular diameter distance respectively [69]. Here the comoving distance at a certain redshift z' is given by

$$\chi(z') = \frac{c}{H_0} \int_0^{z'} \frac{dz}{E(z)}, \quad (2.2)$$

where $E(z)$ denotes the expansion rate of the universe [70], i.e.

$$E(z) = \frac{H(z)}{H_0} = \left[\frac{\Omega_r}{a^4} + \frac{\Omega_m}{a^3} + \frac{\Omega_k}{a^2} + \frac{\Omega_\Lambda}{a^{3(1+w)}} \right]^{1/2}, \quad (2.3)$$

with $a = 1/(1+z)$ standing for the scale factor. Into the above formulae, the property of cosmic neutrinos enters via

$$\Omega_m = \Omega_{\text{DM}} + \Omega_b + \Omega_\nu, \quad (2.4)$$

$$\Omega_r = \Omega_\gamma \left[1 + \frac{7}{8} \left(\frac{4}{11} \right)^{4/3} N_{\text{eff}} \right]. \quad (2.5)$$

Besides Ω_ν and N_{eff} , here Ω_m , Ω_{DM} , Ω_b , Ω_r , Ω_γ , Ω_k , Ω_Λ corresponds to present-day density fractions of all the matter, cold dark matter, baryon, radiation energy, photon energy, curvature, and dark energy, respectively. H_0 is the Hubble constant and c serves as the speed of light.

Cosmic massive neutrinos directly influence the expansion history of the Universe. They also leave their signatures on structure formation and mass distribution, which can be investigated through large scale structure and WL data. To use these data, one needs to know the exact theoretical prediction of the matter power spectrum, i.e. $P(k)$, defined as the Fourier transform of the two-point

correlation function of the matter density contrast $\delta(r) = 1 - \bar{n}(r)/n(r)$. The linear perturbation theory provides reliable results of $P(k)$ at large scales, usually referred to as the linear regime [71–73]. However, as the wavenumber k rises up toward $\sim 0.1 - 0.6$ h/Mpc, the linear perturbation theory starts to break down, and various effects of non-linear clustering take place [74]. The scale-invariant suppression on $P(k)$ caused by massive neutrinos (Eq. 1.2) thus no longer works. Fortunately, people have developed numerous ways to explore those small scale phenomena, e.g. the one-loop perturbation theorem [75–77], which usually takes up the third order expansion of $P(k)$ as a close approximation, the time renormalization group flow method [78], and the most widely quoted HALOFIT analytical formulae as the mapping algorithm calibrated by N-body simulations [79],

$$\Delta^2(k) = \frac{k^3 P(k)}{2\pi} = \Delta_Q^2 + \Delta_H^2, \quad (2.6)$$

where the total power spectrum $\Delta^2(k)$ is split into a quasi-linear term Δ_Q^2 and a pure non-linear term Δ_H^2 . However, three problematic issues are found to affect the neutrino damping effect reproduced by this method [80]:

- (I) HALOFIT overpredicts the suppression in non-linear regime, with maximum discrepancy occurring at $k \sim 1$ h/Mpc;
- (II) HALOFIT cannot capture the redshift dependence of maximum suppression's location in power spectrum;
- (III) at very small scales ($k > 2$ h/Mpc), HALOFIT underpredicts the non-linear power.

Ref. [80] conducted a more extensive suite of N-body simulations particularly designed for quantifying precisely the suppression from massive neutrinos, and improved the original method into HALOFIT- ν algorithm,

$$\Delta'^2(k) = (\Delta_Q'^2 + \Delta_H'^2) \cdot (1 + Q_\nu), \quad (2.7)$$

with both quasi- and non-linear terms modified, and Q_ν accounts for additional non-linear growth of the neutrino component [cf. Ref. 80, appendix A]. For the sake of the accuracy of our constraints, we adopt HALOFIT- ν as the correction to the original $P_{\text{lin}}(k)$ in presence of massive neutrinos, calculated numerically through the hierarchical Boltzmann equations.

2.1 Weak Gravitational Lensing

After the calculations of matter power spectra, under Limber's approximation, the convergence power spectrum of WL can be computed from the integration of matter power spectra along line of sight (see e.g. Ref. [81]),

$$P_l^\kappa = \frac{9H_0^4 \Omega_m^2}{4c^4} \int_0^{\chi_H} \frac{d\chi}{a^2(\chi)} \left[\int_\chi^{\chi_H} d\chi' n(\chi') \frac{r(\chi' - \chi)}{r(\chi')} \right]^2 P\left(\frac{l}{r(\chi)}, \chi\right), \quad (2.8)$$

where $l = k \cdot r(\chi)$ represents the multipole moment and $n(\chi(z))$ accounts for the source redshift distribution. In principle, χ_H should cover the entire Hubble radius, yet we can still safely replace it by $\chi(z_{\text{lim}})$, i.e. the comoving distance out to the survey limited redshift (z_{lim}), where the source normalized number count ($n(z)$) is sufficiently decaying. Since massive neutrinos damp matter power spectrum at small scales, the convergence power of WL is also reduced.

For the actual survey, we choose the published CFHTLS-T0003 observations which have measured about 2×10^6 galaxies with i_{AB} magnitudes between 21.5 and 24.5, imaged on an area of 57 square degree (35 square degree effectively) [82]. CFHTLS-T0003 has provided the community with

the observational results of the shear correlation function $\xi_{E,B}$, the shear top-hat variance $\langle |\gamma|^2 \rangle_{E,B}$, and the aperture-mass variance $\langle M_{\text{ap}}^2 \rangle$. Amongst these three types of WL measurements, $\langle M_{\text{ap}}^2 \rangle$ has the virtue of less systematics prone due to its unambiguous local decomposition [83]. Theoretically, the aperture-mass variance is related to the convergence power spectrum via [84, 85],

$$\langle M_{\text{ap}}^2 \rangle(\theta) = \frac{288}{\pi\theta^4} \int_0^\infty \frac{dl}{l^3} J_4^2(l\theta) P_l^\kappa, \quad (2.9)$$

with $J_\alpha(x)$ being the Bessel function of the first kind. Due to the choice of WL data, we use the following parameterization for the source distribution, as recommended by Ref. [82],

$$n(z) \propto \frac{z^a + z^{ab}}{z^b + c}, \quad (2.10)$$

$$\int_0^{z_{\text{lim}}} n(z) dz = 1,$$

where a , b , and c are nuisance parameters¹ and the survey limited redshift is assigned the value of $z_{\text{lim}} = 7$ (M. Kilbinger, private communication).

2.2 Type Ia Supernovae

The use of SNIa as standardizable candles provides a powerful probe to explore the properties of dark energy. SNIa observations furnish one of the metric distances, i.e. the luminosity distance,

$$D_L(z) = r(z)(1+z) \quad (2.11)$$

where $r(z)$ is the comoving angular diameter distance given by Eq. 2.1. We use the latest Union2.1 compilation of SNIa dataset reported by Ref. [86] in the redshift range $0.015 \leq z \leq 1.414$. This SNIa catalog consists of 580 individual supernova events and is cautiously calibrated against numerous sources of systematic uncertainties. Compared with the former Union2 compilation [87], this updated dataset includes twenty-three new events at high redshifts ($0.6 < z < 1.4$) and thus are helpful in tightening the constraints on the early behavior of dark energy.

Besides the Union2.1 compilation, there are a number of popular SNIa samples, e.g. ESSENCE [88], Constitution [89], SDSS-II [90], SNLS3 [91]. In deriving those datasets, different light curve fitters are adopted. Generally speaking, three independent fitters are proposed and maintained amongst the cosmology community, i.e. SALT2 [92], MLCS2k2 [93], and SiFTO [94]. When trained on the same SNIa data, SALT2 and SiFTO lead to similar cosmological results. However, using the same dataset including SDSS-II, Ref. [90] discovered a difference of 0.2 in the best-fits of w by SALT2 and MLCS2k2, which already exceeds the total error budget (statistical and systematic) contributed from other sources (also see e.g. Ref. [95], where the discrepancy reaches 3σ). Furthermore, it is found that irrespective of which fitter is selected excluding MLCS2k2, different SNIa samples give largely consistent results, however as long as MLCS2k2 is considered, different datasets lead to notably different constraints on Ω_m [96]. The major difference between the MLCS2k2 fitter and the other two originates from the difference in the rest-frame U band region, where the training of MLCS2k2 relies exclusively on nearby SNIa observations while the other two also consider high redshift data [87]. In order to focus on the constraints on neutrino properties, we decide to use the largest sample insofar (i.e. Union2.1) which is obtained from the currently favored and more widely used method (i.e. SALT2). This also allows comparisons with most of other published results.

¹We directly take the best-fit values of a , b , and c presented in Table 2 of Ref. [82]. We have numerically checked that the correlation coefficients between these nuisance parameters and cosmological parameters are trivial enough to be neglected. The similar approach is adopted in Ref. [44].

2.3 Baryon Acoustic Oscillations

As the CMB radiation decouples from the primordial photon-baryon plasma, the features of acoustic oscillations are imprinted onto matter clustering as well and appear as peaks in the galaxy correlation function with a characteristic comoving separation of 100 h/Mpc [97, 98]. Baryon acoustic oscillations (BAO) thus supply us with a standard ruler to measure distances out to the redshift where the bulk of galaxies are observed.

The first detection was achieved by Ref. [99], using SDSS DR3 LRG sample with effective redshift $z = 0.35$. They defined the acoustic parameter which is independent of dark energy models as,

$$A \equiv D_V(z) \frac{\sqrt{\Omega_m H_0^2}}{zc}, \quad (2.12)$$

where the distance combination is depicted by

$$D_V(z) = \left[r^2(z) \frac{zc}{H(z)} \right]^{1/3}, \quad (2.13)$$

with $r(z)$ given by Eq. 2.1. We use the BAO measurements from the surveys of SDSS DR7 [100] and WiggleZ [101]. Hence in total BAO results at five redshifts, i.e. $z = 0.2, 0.35, 0.44, 0.6, 0.73$, are involved in the constraints. Using the earlier SDSS result, Ref. [23] suggested that the inclusion of BAO can help break the degeneracy between dark energy and neutrino masses.

2.4 Observational Hubble Parameter Data

The differential-age technique directly measures the Hubble parameter as

$$H(z) = -\frac{1}{1+z} \frac{dz}{dt}, \quad (2.14)$$

and therefore endowed the OHD with special functionality as standard clocks. The quantity dz/dt is usually determined by measuring the age differences between passively evolving galaxies with nearly the same spectroscopic redshift [50]. We use the most up-to-date datasets summarized by [51], which comprises nineteen OHD measurements over the redshift interval from $0.09 \leq z \leq 1.75$.

2.5 Further Data and Priors

Complementary to late-time large scale probes (including WL) and other standard geometrical indicators (e.g. SNIa, BAO, OHD), the observation of CMB anisotropies is vital in this analysis. We use four independent power spectra, i.e. the temperature auto-power C_l^{TT} , the curl-free component polarization auto-power C_l^{EE} , the curl component polarization auto-power C_l^{BB} , and the T-E cross-correlation C_l^{TE} , at the last scattering surface during the decoupling epoch ($z \sim 1090$). We use the WMAP seven-year data via including the standard pipeline for computing the likelihood, supplied and maintained by the WMAP collaboration². Apart from that, a top-hat prior of $10 \text{ Gyr} < t_0 < 20 \text{ Gyr}$ on the cosmic age is employed. Last but not least, in all data combinations, we always impose the HST prior on the Hubble constant as $H_0 = 74.2 \pm 3.6 \text{ km/s/Mpc}$ [102].

²available at the LAMBDA website, <http://lambda.gsfc.nasa.gov/>

3 Constraints on Cosmological Parameters

The cosmological parameters we use are presented in Table 1. Our most generalized parameter space is composed of the ‘‘Vanilla+Extended’’ sets of parameters, represented by the following vector,

$$\mathbf{P} \equiv (\Omega_b h^2, \Omega_{\text{DM}} h^2, \theta_A, \tau, n_s, \ln(10^{10} A_s), \{\sum m_\nu, N_{\text{eff}}, w\}). \quad (3.1)$$

In addition, the pivot value of the primordial power spectrum is taken to be $k_0 = 0.05 \text{ Mpc}^{-1}$. For simplicity, we assume a flat geometry and purely adiabatic initial conditions. We note that a non-zero curvature might loosen the constraint on $\sum m_\nu$ [103], but the WMAP seven-year result strongly confines $-0.00133 < \Omega_k < 0.0084$ (95% CL), which justifies our assumption. Moreover, we do not consider a running spectral index or any tensor contribution, for the constraint on neutrino masses is not relaxed even when they are allowed [104]. We also do not consider an evolving equation of state.

Our code is a modified version of the publicly available package CosmoMC [105]³. The global fitting to parameter vector \mathbf{P} is achieved through the exploration of the corresponding multidimensional parameter space with the Markov Chain Monte Carlo (MCMC) technique. In realizing the MCMC approach, the Metropolis-Hastings algorithm is implemented to generate sets of chains containing sample points distributed according to the overall likelihood in the parameter space with top-hat prior probability distribution on each input parameter (see Table 1).

Aiming at joint analyses of cosmological probes, we select five combinations from the aforementioned datasets (see Sect. 2), i.e. CMB, CMB+WL, CMB+BAO+OHD, CMB+BAO+SNIa, and CMB+WL+BAO+OHD+SNIa, the last of which is often quoted as the full combination hereafter. For all data combinations, the HST prior is always used. For a progressive and intensive exploration on the extended parameter set, there exist six scenarios for parameter combinations, i.e. Vanilla+ $\sum m_\nu$, Vanilla+ N_{eff} , Vanilla+ $\sum m_\nu+N_{\text{eff}}$, Vanilla+ $w+\sum m_\nu$, Vanilla+ $w+N_{\text{eff}}$, Vanilla+ $w+\sum m_\nu+N_{\text{eff}}$. As a consequence, we have attempted more than thirty runs in total, so as to sample the likelihood distribution in multivariate space for different combinations of observational data. For each run, eight chains are simultaneously generated using parallel computation, and they stop as soon as the criterion of Gelman and Rubin test (R statistics) is satisfied. Generally speaking, after convergence, our chains contain 10^5 points each and guarantee $R - 1 < 0.01$. Then these chains are thinned and joined, left with more than 20000 points for the final constraints on each scenario for each data combination. The details of our results are reported as follows.

3.1 Vanilla+ $\sum m_\nu$

We first explore the parameter space of Vanilla+ $\sum m_\nu$. Our main constraint results are quantitatively summarized in Table 2. Fig. 1 displays the one-dimensional marginalized posterior distribution on some important parameters, while Fig. 2 shows the two-dimensional confidence contours revealing some crucial parameter degeneracies. Here as usual, we assume total degeneracy for the three basic neutrino eigenstates. The effective number of neutrinos is fixed as its standard value, i.e. $N_{\text{eff}} = 3.046$. The constraints are drawn under the context of the popular cosmological constant model ($w = -1$). Like many other papers on constraining $\sum m_\nu$ while fixing N_{eff} and w , we found a 95% CL upper bound on the sum of neutrino masses, $\sum m_\nu < 0.476 \text{ eV}$, using the full combination. (Hereafter we neglect the unit of ‘‘eV’’ for brevity.) This is a 10% improvement over the formerly reported upper limit given by Ref. [45] and Ref. [46] using similar data. The WL evidently contributes to the overall constraints, pushing forward from $\sum m_\nu < 0.524$ (CMB) to $\sum m_\nu < 0.496$ (CMB+WL), even better than the result given by CMB+BAO+SNIa. It reveals one of the greatest advantages of the WL

³<http://cosmologist.info/cosmomc>

technique that it measures the matter fluctuation amplitude very accurately, as seen from Table 2; σ_8 is pinned down to the narrowest 68% confidence range for CMB+WL. Moreover, the OHD give similar, even slightly better results than the SNIa do ($\sum m_\nu < 0.486$ vs. $\sum m_\nu < 0.518$), considering the vast difference between the statistical size of the two data sample (19 vs. 580). This may be persuasive in designing next generation spectroscopic surveys in pursuit of large sample OHD measurements [106, 107]. From Fig. 2, we see a mild proportionality between $\sum m_\nu$ and Ω_m while a slight inverse proportionality between $\sum m_\nu$ and H_0 is also seen. The inverse proportionality between $\sum m_\nu$ and σ_8 should be counted as the strongest correlation. Those degeneracies naturally explain why our best-fit values for Ω_m , H_0 and σ_8 are mildly larger, a little smaller, and unambiguously smaller than the WMAP seven-year recommended values. Except for the three derived parameters, constraints on the Vanilla parameter set retrieve nearly the same results as reported by the WMAP seven-year analysis. In particular, including additional probes does not result in much better constraints on n_s and the degeneracy between $\sum m_\nu$ and n_s is marginal, since the variation of n_s changes the global shape of matter power spectrum whereas $\sum m_\nu$ only damps $P(k)$ at small scales.

3.2 Vanilla+ N_{eff}

Then we test the scenario of Vanilla+ N_{eff} against each cosmological data combination. Likewise, the main results are presented in Table 3, Fig. 3 (one-dimensional) and Fig. 4 (two-dimensional). Here the global fitting is completed under the assumption of massless neutrino with Λ CDM cosmology. Using the full combination of cosmological probes, we obtain $N_{\text{eff}} = 3.271 \pm 0.367$, which rules out additional light degrees of freedom at nearly 95% CL. This result is in support of the standard prediction of big bang nucleosynthesis, and is primarily due to the contribution of the WL data ($N_{\text{eff}} = 3.334 \pm 0.496$ for CMB+WL, whereas $N_{\text{eff}} = 4.340 \pm 0.817$ for CMB alone). The OHD also tend to favor the standard value. Including OHD, we obtain $N_{\text{eff}} = 3.722 \pm 0.418$, which is fully consistent with Ref. [51] ($N_{\text{eff}} = 3.7 \pm 0.4$). Once again OHD give rather tighter bounds on the effective number of neutrinos than the SNIa do, and this time the difference between their constraining powers is more clearly revealed. The SNIa data seem to prefer the largest N_{eff} best-fit value with the largest uncertainty. In this case, the inclusion of the SNIa data does not improve the constraint on either H_0 or $\Omega_{\text{DM}}h^2$. Fig. 4 displays several parameter correlations. As reported by Ref. [61], we see the strong anticorrelation between N_{eff} and $\Omega_{\text{DM}}h^2$. The degeneracy between N_{eff} and H_0 is also remarkably strong. The propotional trend between N_{eff} and Ω_m is mild and disappears when the full combination is employed. These correlations arise from the role N_{eff} plays in the radiation content, which decides the epoch of matter-radiation equality as

$$1 + z_{\text{eq}} = \frac{\Omega_m}{\Omega_r} = \frac{\Omega_m h^2}{1 + 0.2271 N_{\text{eff}}} (\Omega_\gamma h^2)^{-1}. \quad (3.2)$$

CMB measures precisely the present-day photon energy density to be $\Omega_\gamma h^2 = 2.469 \times 10^{-5}$ for $T_{\gamma 0} = 2.725$ K [9]. Given the rather narrow range of $z_{\text{eq}} = 3141_{-157}^{+154}$ [70], Eq. 3.2 thereby explains the correlations observed between N_{eff} , Ω_m , and H_0 . The degeneracy between N_{eff} and $\Omega_{\text{DM}}h^2$ is also extracted from Eq. 3.2, since $\Omega_m h^2 = \Omega_b h^2 + \Omega_{\text{DM}} h^2$ and meanwhile the physical baryon density $\Omega_b h^2$ is tightly constrained by the CMB observations. Unlike its inverse proportionality with $\sum m_\nu$, σ_8 shows clear proportionality with N_{eff} . Because the observation of WL provides an accurate and independent measurement on σ_8 , we thus expect that WL plays the most influential role in current constraints. The inclusion of SNIa is inadequate to deal with parameter degeneracies associated with N_{eff} , and that is the reason for some of the poor constraints given by CMB+BAO+SNIa. Like the scenario of Vanilla+ $\sum m_\nu$, the constraints on the Vanilla parameter set are similar to the WMAP seven-year results. and the degeneracy between N_{eff} and n_s is broken when all data are included.

3.3 Vanilla+ $\sum m_\nu$ + N_{eff}

We next investigate the case when both $\sum m_\nu$ and N_{eff} are set free, under the assumption of cosmological constant. Our main constraints are presented in Table 4, Figs. 5 and 6. Undoubtedly, the inclusion of N_{eff} as a free parameter tremendously weakens the constraints on $\sum m_\nu$. Interestingly, when the full combination is considered, a robust 68% lower limit is revealed and our result is $\sum m_\nu = 0.421^{+0.186}_{-0.219}$ at 68% CL. Nonetheless, considering that the best-fit of our current result is almost excluded at 95% CL by our former constraint when N_{eff} is fixed ($\sum m_\nu < 0.476$), this may illustrate our worry on the robustness of all stringent upper bounds on $\sum m_\nu$ ever reported in previous literature. The constraints on N_{eff} are also relaxed due to the freedom on $\sum m_\nu$. Unlike former results, the extra neutrino species is slightly favored, as our best constraint reads $N_{\text{eff}} = 3.740 \pm 0.446$. The WL data still shows great promise as it refines the constraints from ($\sum m_\nu < 1.515$, $N_{\text{eff}} = 5.729 \pm 1.274$, CMB alone) to ($\sum m_\nu < 1.393$, $N_{\text{eff}} = 4.308 \pm 0.924$, CMB+WL), mainly due to its precise constraint on σ_8 . The combination of CMB+BAO+OHD(+HST) (Fig. 6) exerts more dominant influence on the parameter constraints, as the cyan and magenta contours are more alike. Besides the enormous information from the WMAP seven-year data, the OHD+HST delivers direct knowledge on the expansion history. In combination with the BAO distance indicator, this combination therefore is capable of successfully breaking several hard parameter degeneracies, e.g. ($\sum m_\nu$ vs. H_0), (N_{eff} vs. Ω_m). However even against the full combination, some correlations of parameters still remain. For instance, a larger $\sum m_\nu$ value shows a preference for a smaller σ_8 yet a slightly larger Ω_m , whereas a larger N_{eff} favors a larger $\Omega_{\text{DM}}h^2$ and/or H_0 . Most importantly, the mild proportionality between ($\sum m_\nu$, N_{eff}) reasonably points to the fact that a larger total neutrino mass is preferred by a larger effective number. As an increasing number of observations infer extra light degrees of freedom, varying $\sum m_\nu$ and N_{eff} simultaneously will be a non-trivial consideration to derive constraints on both $\sum m_\nu$ and N_{eff} . As in previous scenarios, the constraints on the Vanilla parameter set are mostly unaffected.

3.4 Vanilla+ w + $\sum m_\nu$

The previous stage of our analysis is constructed under the hypothesis of the cosmological constant being the underlying dark energy model. In what follows, we shall assume the dark energy component has a variable EOS, w . The other free extended parameter is $\sum m_\nu$. The main results for this scenario are shown in Table 5, Figs. 7 and 8. Owing to the inclusion of w as a free parameter, the best constraint on the sum of neutrino masses relaxes to $\sum m_\nu < 0.627$ (with no lower limit observed). In this scenario, the primary predominance the SNIa data holds over the OHD is demonstrated, i.e. the special importance of the SNIa data in constraining w . In practice, the SNIa impose much tighter constraint ($w = -1.074 \pm 0.088$) than the OHD ($w = -1.240 \pm 0.182$). Due to the degeneracy between w and $\sum m_\nu$, CMB+BAO+SNIa thus presents better result ($\sum m_\nu < 0.688$) than CMB+BAO+OHD gives ($\sum m_\nu < 0.819$). Moreover, the combination of CMB+BAO+SNIa furnish an overallly stringent constraint, as the green contours almost overlap with the cyan ones shown in Fig. 8. Besides, adding the present WL data does not help much at improving the constraints when w is allowed to vary freely. Although the technique of WL has been forecasted to be a promising tool to discriminate between dark energy and neutrino masses [41], currently speaking the WL data do not provide this discerning ability, albeit its constraint on σ_8 is still incomparable. The anticorrelation between $\sum m_\nu$ and σ_8 is strong as usual, while $\sum m_\nu$ and w are found to be highly correlated. Nevertheless, the degeneracies between $\sum m_\nu$, Ω_m and H_0 are mild. Especially, the inclusion of the SNIa data manages to break the degeneracy of (Ω_m vs. w).

3.5 Vanilla+ w + N_{eff}

The next parameter scenario to explore is Vanilla+ w + N_{eff} . Table 6, Figs. 9 and 10 present the main results. Unlike the great impact varying w exerts on the $\sum m_\nu$ constraints, the best constraint on N_{eff} is only compromised a little by freeing w , which reads $N_{\text{eff}} = 3.454 \pm 0.386$. But the inclusion of the free EOS parameter does make the combination of CMB(+HST) lose their capability to derive a reliable upper limit on N_{eff} . However the importance of WL reappears unlike the case of Vanilla+ w + $\sum m_\nu$; the WL data constrains $N_{\text{eff}} = 3.192 \pm 1.214$. Here the OHD wields incomparable constraining power on the effective number of neutrino species, i.e. $N_{\text{eff}} = 3.623 \pm 0.432$, whereas the SNIa luminosity distance measurements still overpredict N_{eff} to an exceedingly large value. On w , the SNIa data without the contributions of WL or OHD strongly constrain $w = -0.986 \pm 0.077$. In Fig. 10, interesting features again show up. The proportionality between N_{eff} and $\Omega_{\text{DM}}h^2$ is always strong and impossible to suppress. The degeneracy between N_{eff} and Ω_{m} is broken when the full combination is employed. The correlation between N_{eff} and H_0 is present, yet weak. Particularly, the degeneracy directions between N_{eff} and w , given by CMB+BAO+OHD and CMB+BAO+SNIa, show a nearly orthogonal feature. It is thereby enlightening since the OHD have the advantage of better constraining N_{eff} while the SNIa are capable of pinning down w more precisely. So when the OHD and the SNIa are combined, it is easy to break the degeneracy between N_{eff} and w , as shown in our plots.

3.6 Vanilla+ w + $\sum m_\nu$ + N_{eff}

Finally, the most generalized scenario, where all of the three extended parameters are free to vary, is analyzed. Our main results are given in Table 7, Figs. 11 and 12. The best-fits give $\sum m_\nu = 0.556^{+0.231}_{-0.288}$, $N_{\text{eff}} = 3.839 \pm 0.452$, and $w = -1.058 \pm 0.088$. Once again a 68% CL lower limit for $\sum m_\nu$ is robustly observed. As discussed in previous scenarios, the WL data contribute most to the constraint on σ_8 , and the narrowest 68% confidence intervals of w and Ω_{m} result from the inclusion of the SNIa data. In addition, due to the degeneracy of ($\sum m_\nu$ vs. w), the SNIa offer better constraint on $\sum m_\nu$ than the OHD. However, concerning N_{eff} , it is still the OHD that provide the most strict constraint. Moreover, it is found that for various scenarios, when N_{eff} is kept free, CMB+BAO+SNIa presents much weaker constraints on $\Omega_{\text{DM}}h^2$ than CMB+BAO+OHD, yet their constraints look similar otherwise. This is a straightforward consequence of Eq. 3.2. Since CMB+BAO+OHD delivers direct information on the expansion history, it provides the most stringent constraint on $\Omega_{\text{DM}}h^2$. As seen from Fig. 12, when the entire set of extended parameters are freed, some of the parameter correlations turn mild, e.g. (N_{eff} vs. H_0) and ($\sum m_\nu$ vs. w). Nevertheless, the degeneracies of ($\sum m_\nu$ vs. σ_8) and (N_{eff} vs. $\Omega_{\text{DM}}h^2$) are persistent. Once again the confidence contours of (N_{eff} vs. w) display remarkable features: CMB+BAO+OHD and CMB+BAO+SNIa impose strict constraints with nearly orthogonal degeneracy directions, which emphasizes the importance of combining OHD and SNIa in future studies. Albeit mild, the proportion between $\sum m_\nu$ and N_{eff} still exists. It again implies that one should vary $\sum m_\nu$ and N_{eff} simultaneously in order to obtain more reliable constraints on cosmic relic neutrino properties.

We note that within most scenarios, the best-fit values of σ_8 are slightly low compared with the observations of galaxy clusters or Ly α forest [21, 108]. However we argue that the results are strongly affected by the anticorrelation between $\sum m_\nu$ and σ_8 . In our trial run with all the extended parameters fixed at their standard values, i.e. the usual Λ CDM scenario, we obtain $\sigma_8 = 0.791 \pm 0.018$ and $\Omega_{\text{m}} = 0.255 \pm 0.015$, which are in total agreement with Ref. [83].

4 Neutrino Impact on Structure Formation

Over thirty sets of constraint results have been presented and discussed. In order to understand the physical origins underneath those parameter degeneracies, we investigate specifically the influences of the three extended parameters on growth of perturbation and formation of structures. We calculate a variety of matter power spectra via the CAMB code [109]⁴ with the HALOFIT- ν algorithm [80]. Here the default parameter set (“ALL”) refers to the best-fit values of the Vanilla+ $w+\sum m_\nu+N_{\text{eff}}$ scenario against the full data combination (see Table 7). Hereafter, for simplicity, we assume total degeneracy for the standard three eigenstates of neutrinos, with mass for each flavor given by $m_\nu = (\sum m_\nu)/3$.

As mentioned in Sect. 1, massive neutrinos influence structure formation due to their large thermal velocity dispersion [110]

$$\sigma_\nu(z) = \sqrt{\frac{15\zeta(5)}{\zeta(3)} \frac{T_\nu(z)}{m_\nu}}, \quad (4.1)$$

where $\zeta(s)$ denotes the Riemann zeta function, and T_ν represents the neutrino temperature, which can be associated with the present-day temperature for the CMB, i.e. $T_\nu(z) = (4/11)^{1/3} T_{\gamma 0}(1+z)$. This kinematic activity, i.e. the effect of free-streaming, prevents neutrinos from clustering below the free-streaming scale, and thus ensures the density perturbation of neutrinos below this scale negligible. By analogy with the Jeans length, this characteristic redshift-dependent scale is defined as [111],

$$k_{\text{FS}}(z) = \sqrt{\frac{3}{2}} \frac{H(z)}{(1+z) c_{s,\nu}(z)}, \quad (4.2)$$

with $H(z)$ given by Eq. 2.3, and $c_{s,\nu}$ being the sound speed for thermalized neutrinos, which can be strictly related to the velocity dispersion through $c_{s,\nu} = \frac{\sqrt{5}}{3} \sigma_\nu$, in the non-relativistic limit [112]. Neutrinos become non-relativistic when their energy density $\langle E \rangle = \frac{7\pi^4}{180\zeta(3)} T_\nu = m_\nu$, and this transition occurs at $1+z_{\text{NR}} \sim 1890(m_\nu/1 \text{ eV})$. Therefore for masses smaller than $\sim 0.6 \text{ eV}$ (the HALOFIT- ν algorithm is well calibrated within this mass range), neutrinos will not dramatically slow down until the last scattering of photons ceases. Apart from that, if the neutrinos are massive enough, i.e. $m_\nu > 0.005 \text{ eV}$, to have decelerated before dark energy dominates the expansion history, the Hubble horizon at the epoch when they turn into non-relativistic can be described by [110],

$$k_{\text{NR}} = \frac{H(z_{\text{NR}})}{1+z_{\text{NR}}} \sim 0.0145 \left(\frac{m_\nu}{1 \text{ eV}} \right)^{1/2} \Omega_{\text{m}}^{1/2} \text{ h/Mpc}. \quad (4.3)$$

This is the largest scale where the presence of finite-mass neutrinos starts to influence low-redshift matter power spectra by the free-streaming effect; above this scale, massive neutrinos can be treated simply as aggregating CDM. At scales $k > k_{\text{NR}}$, neutrinos not only free-stream to erase their fluctuations, but also damp the amplitude of the total matter power spectra by at least a few percent.

We first display the signatures of massive neutrinos on matter power spectra at redshift $z = 0, 1, 3$, in Fig. 13. From Panel (a), as neutrinos become heavier, the suppression is increasingly severe at small scales, with the maximum suppression in the non-linear regime represented roughly by $\Delta P/P \sim -9.8 (\Omega_\nu/\Omega_{\text{m}})$ [113]. The redshift-dependence of the maximum suppression is analytically captured by the HALOFIT- ν mapping algorithm [80]. From a crude glance at Panel (b), as more extra light degrees of freedom are introduced, matter power at small scales are more damped as well.

⁴<http://camb.info/>

Under more cautious inspection, the acoustic peaks are meanwhile shifted to smaller scales. We attempt to interpret these results in what follows.

With a fixed total matter density $\Omega_m h^2$, the increase of N_{eff} will postpone matter-radiation equality (see Eq. 3.2). Since at subhorizon scales, the matter perturbations grow more efficiently during the matter-dominated epoch rather than during the radiation-dominated epoch, it is reasonable to deduce that the matter power spectrum is more severely damped at small scales relatively to large scales, which is one of the most pronounced features displayed in Fig. 13(b). For CMB, this effect is opposite; the height of the first acoustic peak is increased, mainly through the early integrated Sachs-Wolfe effect [114]. On the contrary, for the third and higher order peaks, the amplitudes are more damped due to the free-streaming of ultrarelativistic neutrinos [115]. The position of the n th acoustic peak can be estimated by $l_n \sim n\pi/\theta_A$, with the acoustic scale parameter defined as (also see Table 1),

$$\theta_A = \frac{s(z_{\text{dec}})}{r(z_{\text{dec}})}, \quad (4.4)$$

where r is given by Eq. 2.1 and $z_{\text{dec}} \sim 1090$ signals the epoch of photon-baryon decoupling [116]. Furthermore, z_{dec} is insensitive to the presence of massive neutrinos and $r(z_{\text{dec}})$ almost remains unaltered for different values of N_{eff} [117]. Usually, the sound horizon is calculated via [73],

$$s(z) = \int_0^{1/(1+z)} c_s(a) \frac{da}{a^2 H(a)}, \quad (4.5)$$

with the sound speed for the photon-baryon fluid $c_s^2 = c^2/[3(1+R)]$ and $R = (3\Omega_b/4\Omega_\gamma)a$. Since the massive neutrinos we are interested in maintain their relativistic speed before the recombination epoch, it is reasonable to conjecture that every neutrino species can be counted as a part of the radiation during that period. By increasing (decreasing) the value of N_{eff} , equivalently $H(a)$ is changed according to Eq. 2.3, and the sound horizon at the time of decoupling, which dictates the position of the acoustic peaks, is thereby shrunk (enlarged). As a consequence, the acoustic peaks are shifted to smaller (larger) scales, corresponding to larger (smaller) wavenumbers of the matter power spectrum, particularly shown in Fig. 13(b). This feature, which is unique to the variation of N_{eff} , might provide a smoking gun signature for the existence of extra light degrees of freedom.

Unlike the impacts from $(\sum m_\nu, N_{\text{eff}})$, the effect introduced by varying w is a global change of magnitude for the matter power spectrum shown in Fig. 13(c). As inferred from Eq. 2.3, a larger value for w enables the dark energy to present itself with a non-vanishing amount in earlier stage of the expansion history. It thereby explains why the dotted curves in Fig. 13(c), corresponding to matter power spectra at redshift $z = 3$, are almost immune against the decrease of w deviating from -1 . The change of w directly modifies the expansion history, it is therefore reasonable that the matter power at every scale is simultaneously enhanced/reduced. In addition, as shown, the redshift-dependence of maximum suppression is still captured by the fitting algorithm of HALOFIT- ν . Although the original HALOFIT mapping is only calibrated for the Λ CDM cosmological model, through appropriate modifications of the growth function [118] or a specific fitting prescription developed by Ref. [119], one can reliably quantify the non-linear effect of varying w , accurate to a few percent.

Fig. 14 presents the WL convergence power spectra as calculated from Eq. 2.8, with each panel corresponding to the panels of Fig. 13. No wonder the convergence power spectrum is also reduced by the increase of $\sum m_\nu$ and N_{eff} , or the decrease of w , since it is given by the integration of matter power spectra along the line of sight. After integration, we have lost the unique signature for N_{eff} . Fortunately, the impact from w still holds the different behavior of a global change, which can be used to differentiate from the effects introduced by $\sum m_\nu$ and N_{eff} . The maximum suppression on the convergence power is at $l \sim 10^3$, insensitive to the variations of the three parameters. Besides, we

also plot the result predicted by the linear perturbation theory in Fig. 2.8(a). The primary discrepancy takes place below the scale corresponding to $l > 10^2$, and it thereby illustrates the importance of an accurate knowledge of the full non-linear matter power spectrum, for future WL surveys to achieve their full potential [120].

Eventually, the numerical results of the aperture-mass variance given by Eq. 2.9 are demonstrated in Fig. 15, together with the actual data of CFHTLS-T0003. From Panel (a), we see that the current detection of WL signals mainly lies within the semi- to non-linear regime, where the non-linear modeling of matter clustering is vital for a precise interpretation of the observational data. As repeatedly mentioned, the HALOFIT- ν algorithm has great advantages itself, yet the effects of baryons are not covered. The hot baryons harbored within intracluster medium have been shown to affect the WL shear power spectrum up to ten percent at $k \sim 10$ h/Mpc [121]. If sufficiently strong AGN feedback is included, ten percent is already reached at $k \sim 1$ h/Mpc [122]. Using hydrodynamic simulations with consideration of baryon physics, Ref. [123] discovered that as much as 40 percent bias in the constraint on dark energy EOS can be introduced by ignoring the effects of baryons. However, most of the baryon contribution is at smaller scales than currently observed. Besides, finite-mass neutrinos exert quite different impacts on matter clustering compared with the baryons. Thus using current optimal mapping algorithm, HALOFIT- ν , will suffice for the constraints on $\sum m_\nu$. In the precision analysis of the WL, not only are the theoretical prescriptions crucial, but the data quality is also influential. As shown in Fig. 15, a small bump is present around the semi-nonlinear scales in the CFHTLS data. Although $\langle M_{\text{ap}}^2 \rangle$ is a more localized filter and thus less prone to large scale systematics or E-/B-mode mixing, this feature is still mainly caused by some thorny systematic issues, e.g. shape measurements, intrinsic alignments, PSF anisotropies, catastrophic photo- z error. For a thorough discussion on WL systematics, observables and their interplay, we refer the reader to Ref. [124]. Anyhow, the community is looking forward to better settlement of these systematics, in the final release of CFHTLS lensing data in the near future.

5 Conclusion and Discussion

In this paper, we present a comprehensive analysis of the constraints on the sum of neutrino masses, the effective number of neutrino species, and the constant EOS parameter of dark energy. Via employing the most recent observational data of CMB+WL+BAO+OHD+SNIa, we have pinned down the total neutrino mass to $\sum m_\nu < 0.476$ at 95% CL, whereas the constraint reads $\sum m_\nu = 0.421^{+0.186}_{-0.219}$ (68% CL) when N_{eff} is simultaneously set loose, and even gives $\sum m_\nu = 0.556^{+0.231}_{-0.288}$ (68% CL) if w is also included as a free parameter. Given that we only consider the constant EOS for the dark energy in present work, the results including evolving dark energy component will provide even less stringent constraints. This highlights our concern that in constraining neutrino masses using cosmological probes, one needs to take into consideration the correlations between $(\sum m_\nu, N_{\text{eff}}, w)$ seriously. For the effective number parameter, we obtained the best constraints as $N_{\text{eff}} = 3.217 \pm 0.367$ (with fixed $\sum m_\nu$ and w), $N_{\text{eff}} = 3.740 \pm 0.446$ (with freed $\sum m_\nu$ and fixed w), $N_{\text{eff}} = 3.454 \pm 0.386$ (with fixed $\sum m_\nu$ and freed w), and $N_{\text{eff}} = 3.839 \pm 0.452$ (with both $\sum m_\nu$ and w freed). For the most generalized parameter scenario, the standard model of $N_{\text{eff}} = 3.046$ is compatible at 1.75σ CL. If statistical uncertainties were dominating, which is probably true for the BAO and OHD, then we can rule out the standard three flavor neutrinos model at 5σ CL, when the future datasets over eight times as large as current samples are obtained. But for some probes like SNIa, systematics are already dominating, so the expected improvements are not easily estimated. Most probably in the future, equivalent or improved constraints will be obtained with BAO angular diameter distances and Hubble parameter measurements. The constraints on the EOS parameter all along favor the cosmological constant

model, regardless of whether or not varying $\sum m_\nu$ and/or N_{eff} . That is mainly due to the effectiveness of the SNIa data. Moreover, the OHD still provide helpful improvements on dark energy constraints. We also pay particular attention to parameter degeneracies. The strong correlation between N_{eff} and H_0 (also N_{eff} and $\Omega_{\text{DM}}h^2$) can be explained by the rather certain epoch for matter-radiation equality. The strong anticorrelation found in $(\sum m_\nu \text{ vs. } \sigma_8)$ results from the suppression of matter perturbation growth ascribed to the presence of finite-mass cosmic neutrinos. As shown in Sect. 3, due to the different proportionality trends that $\sum m_\nu$ and N_{eff} hold with respect to σ_8 , as well as the advantage of WL in measuring σ_8 , the technique of WL does show great potential in discriminating between the effects of $\sum m_\nu$ and N_{eff} for future large surveys.

Another key aspect in our work is the investigation on the constraining capabilities of different cosmological probes. The WL observation at current stage does contribute to some improvement if the dark energy parameter is fixed. However when w is free to vary, adding the WL data does not result in much better constraints on $\sum m_\nu$. Perhaps the WL tomography and its cross-correlation with other tomographic probes will help improve this situation [42, 43]. On the comparison between the results from the inclusions of OHD and SNIa, it is found that for the constraints on $\sum m_\nu$, when dark energy EOS is fixed ($w = -1$), the result given by OHD is similar to that by SNIa luminous distances or BAO angular diameter distances, with OHD slightly better. If N_{eff} is set free, OHD distinctly prevail over SNIa. Nevertheless, as long as w is freed, the SNIa data confine $\sum m_\nu$ more strictly than the OHD do. Concerning the constraints on the Hubble constant, when only $\sum m_\nu$ is set loose, the SNIa data provide similar constraints as the OHD do. Once N_{eff} is varying, the OHD perform much better than the SNIa, due to the overwhelming power of the OHD in constraining N_{eff} . Additionally, the SNIa and the OHD provide almost the same constraints on Ω_m . On the degeneracy between N_{eff} and w , the inclusions of OHD and SNIa lead to nearly orthogonal degeneracy directions, as explained by their specific powers in constraining N_{eff} and w , respectively. As a consequence, their union will facilitate the breaking of this parameter degeneracy so well that our global constraints on all cosmological parameters will benefit.

The tantalizing indication of a non-zero total neutrino mass is really interesting (see Sec. 3.3 and Sec. 3.6). We argue this is the result of the combined effect from all cosmological probes in our study. First of all, due to the large parameter space and the fact that some parameters, e.g. $\Omega_b h^2$ and τ , are badly constrained by other probes, the CMB data are indispensable, yet not enough even when combined with the H_0 prior. The WL technique provides plenty of information on mass distribution and matter clustering, which are sensitive to the neutrino total mass, however its use is limited by measurement errors as well as the inclusion of variable w . Although not directly related to neutrino masses, the late-time probes, i.e. BAO, SNIa and OHD, are particularly helpful in disentangling some parameter degeneracies. Thereby combining all the observations together, i.e. CMB+WL+BAO+OHD+SNIa(+HST), we can constrain $\sum m_\nu$ very precisely and even impose a 68% CL lower limit. As also pointed out recently by Ref. [125], neither future CMB experiment or weak lensing shear measurement or galaxy tomographic survey alone can reach $\sim 5\sigma$ detection of a non-zero sum of neutrino masses; it is their joint analysis that effectively breaks parameter degeneracies.

The different impacts that dark energy, cosmic neutrino total mass and effective number exert onto matter clustering and structure formation are also discussed. Regarding the effects on low-redshift matter power spectra, the increase of w tends to reduce the global magnitude of matter power at all scales, due to direct modification of the expansion law. On the contrary, the change in $\sum m_\nu$ and/or N_{eff} only affects the power spectrum at scales $k > k_{\text{NR}}$. The increase of $\sum m_\nu$ damps more severely the non-linear matter power due to the free-streaming effect, while the increment on N_{eff} causes delay to the matter-radiation equality epoch, and thus suppresses the growth of matter pertur-

bation at small scales. The suppression caused by N_{eff} is nearly redshift-independent for $k < 1 \text{ h/Mpc}$.

In addition, we note a unique feature of N_{eff} : its variation is capable of shifting acoustic peaks in late-time matter power spectra. Accordingly, the WL convergence power spectrum is altered, and the aperture-mass variance affected. It is also discussed that the precision analysis of WL demands the accurate knowledge of the full non-linear matter power spectrum and the next stage cosmological simulations had better take gas dynamics into account. Albeit the current data of CFHTLS still suffer from systematics, high hope and great endeavor have been invested in this program, which will finally promote our knowledge on the formation and evolution of cosmic structure through WL.

Recently, Ref. [126] tested the model of eV mass scale sterile neutrinos, employing two different SNIa datasets given by different light curve fitters, i.e. Union2 with SALT2, and SDSS-II with MLCS2k2. They found that such sterile neutrino model is strongly supported by the SNIa sample of SDSS-II with MLCS2k2 (~ 55 times more probable than the null model), whereas disfavored by the Union2 SNIa data with SALT2, as well as other cosmological probes. This is not entirely unexpected since several studies have already shown that MLCS2k2 seems to support more exotic physics rather than the Λ CDM model, whereas the very same data standardized with SALT2 are fairly consistent with cosmological constant as well as other types of cosmological observations [96, 127, 128]. We note that in judging the viability of Ref. [126]’s sterile neutrino model, the different fitters do play a role, but also the different SNIa data samples and the estimates of the systematic errors associated with the samples. Therefore to conclude that the light curve fitter is the key factor of vindicating such sterile neutrino model or not, more work should be dedicated to the re-fitting of the same SNIa dataset, especially Union2.1, using different methods.

Cosmological probes we have discussed are mainly sensitive to the sum of neutrino masses, yet almost blind to mass splitting scenarios, if any, for different neutrino eigenstates. Fortunately, cosmological observations can reliably rule out total degeneracy between the eigenstates if $\sum m_\nu$ is constrained *robustly* to be less than 0.22 eV, and furthermore nail down the Normal Hierarchy scenario as the true mass splitting when $\sum m_\nu < 0.1 \text{ eV}$ is *conservatively* derived [cf. Ref. 129, Figure 1].

However, as shown in Fig. 15, these small values for $\sum m_\nu$ are seemingly disfavored by the $\langle M_{\text{ap}}^2 \rangle$ data alone, as the constraint on N_{eff} tends (slightly) to prefer additional light degrees of freedom. In practice, there have been some arguments on discriminating the neutrino mass hierarchy within the framework of Fisher formalism [130–133]. Ref. [134] conducted N-body simulations to study separately the effects from different mass hierarchies and obtained a $\sim 0.5\%$ difference. This small, yet non-trivial result underlines its measurable potential from upcoming space surveys (e.g. Euclid), in combination with ground-based experiments. In our present analyses, N_{eff} is treated as the effective number of neutrinos. We do realize that except members of the neutrino family, other more exotic candidates, e.g. axions, gravitinos, or even primordial magnetic fields, can equally fill for this extra relativistic component. Besides, early dark energy has been shown to be able to reconcile the standard model of three families of neutrinos with various cosmological observations [67]. Nonetheless, as large scientific programs are already providing new results, we are confident that the truth of dark radiation will soon be unveiled.

Acknowledgments

CFHTLS is based on observations obtained with MEGAPRIME/MEGACAM, a joint project of CFHT and CEA/DAPNIA, at the Canada-France-Hawaii Telescope (CFHT) which is operated by the National Research Council (NRC) of Canada, the Institut National des Sciences de l’Univers of the Centre National de la Recherche Scientifique (CNRS) of France, and the University of Hawaii. This work is based in part on data products produced at TERAPIX and the Canadian Astronomy Data Centre

as part of the Canada-France-Hawaii Telescope Legacy Survey, a collaborative project of NRC and CNRS. We acknowledge the use of the Legacy Archive for Microwave Background Data Analysis (LAMBDA). Support for LAMBDA is provided by the NASA Office of Space Science. The use of the user-friendly and freely available package CosmoMC and CAMB is also warmly acknowledged. The numerical calculations in this paper have been done on the IBM Blade cluster system in the High Performance Computing Center (HPCC) of Nanjing University.

The useful suggestions from the anonymous referee are greatly appreciated. We are deeply grateful to the helpful conversations with Hao Wang, Qiao Wang, Cong Ma, Lei Sun, You-Hua Xu, Shuo Yuan, Jun-Qing Xia, Gong-Bo Zhao, Hu Zhan, Hong Li, Liang Cao, Shahab Joudaki, Martin Kilbinger, Philip Marshall, Richard Shaw, and Joop Schaye. We thank Antony Lewis for technical support on cosmocoffee⁵. This work was supported by the National Science Foundation of China (grant No. 11173006), the Ministry of Science and Technology National Basic Science program (project 973) under grant No. 2012CB821804, the Fundamental Research Funds for the Central Universities, the National Natural Science Foundation of China (Grant No. 11033002) and the National Basic Research Program of China (973 Program, Grant No. 2009CB824800).

References

- [1] M. Maltoni, T. Schwetz, M. Tórtola, and J. W. F. Valle, *Status of global fits to neutrino oscillations*, *New Journal of Physics* **6** (Sept., 2004) 122, [[hep-ph/04](#)].
- [2] S. Hannestad, *Primordial Neutrinos*, *Annual Review of Nuclear and Particle Science* **56** (Nov., 2006) 137–161, [[hep-ph/06](#)].
- [3] C. Kraus, B. Bornschein, L. Bornschein, J. Bonn, B. Flatt, A. Kovalik, B. Ostrick, E. W. Otten, J. P. Schall, T. Thümmler, and C. Weinheimer, *Final results from phase II of the Mainz neutrino mass search in tritium β decay*, *European Physical Journal C* **40** (Apr., 2005) 447–468, [[hep-ex/04](#)].
- [4] H. V. Klapdor-Kleingrothaus, A. Dietz, L. Baudis, G. Heusser, I. V. Krivosheina, B. Majorovits, H. Paes, H. Strecker, V. Alexeev, A. Balysh, A. Bakalyarov, S. T. Belyaev, V. I. Lebedev, and S. Zhukov, *Latest results from the HEIDELBERG-MOSCOW double beta decay experiment*, *European Physical Journal A* **12** (2001) 147–154, [[hep-ph/01](#)].
- [5] S. Hannestad, *Neutrino physics from precision cosmology*, *Progress in Particle and Nuclear Physics* **65** (Oct., 2010) 185–208, [[arXiv:1007.0658](#)].
- [6] K. N. Abazajian, E. Calabrese, A. Cooray, F. de Bernardis, S. Dodelson, A. Friedland, G. M. Fuller, S. Hannestad, B. G. Keating, E. V. Linder, C. Lunardini, A. Melchiorri, R. Miquel, E. Pierpaoli, J. Pritchard, P. Serra, M. Takada, and Y. Y. Y. Wong, *Cosmological and astrophysical neutrino mass measurements*, *Astroparticle Physics* **35** (Nov., 2011) 177–184, [[arXiv:1103.5083](#)].
- [7] J. Lesgourgues and S. Pastor, *Massive neutrinos and cosmology*, *Phys. Rept.* **429** (July, 2006) 307–379, [[astro-ph/](#)].
- [8] S. Dodelson, E. Gates, and A. Stebbins, *Cold + Hot Dark Matter and the Cosmic Microwave Background*, *Astrophys. J.* **467** (Aug., 1996) 10, [[astro-ph/](#)].
- [9] E. Komatsu, K. M. Smith, J. Dunkley, C. L. Bennett, B. Gold, G. Hinshaw, N. Jarosik, D. Larson, M. R.olta, L. Page, D. N. Spergel, M. Halpern, R. S. Hill, A. Kogut, M. Limon, S. S. Meyer, N. Odegard, G. S. Tucker, J. L. Weiland, E. Wollack, and E. L. Wright, *Seven-year Wilkinson Microwave Anisotropy Probe (WMAP) Observations: Cosmological Interpretation*, *Astrophys. J. Suppl.* **192** (Feb., 2011) 18, [[arXiv:1001.4538](#)].
- [10] J. Lesgourgues, L. Perotto, S. Pastor, and M. Piat, *Probing neutrino masses with CMB lensing extraction*, *Phys. Rev. D* **73** (Feb., 2006) 045021, [[astro-ph/](#)].

⁵<http://cosmocoffee.info>

- [11] D. Baumann, M. G. Jackson, P. Adshead, A. Amblard, A. Ashoorioon, N. Bartolo, R. Bean, M. Beltrán, F. de Bernardis, S. Bird, X. Chen, D. J. H. Chung, L. Colombo, A. Cooray, P. Creminelli, S. Dodelson, J. Dunkley, C. Dvorkin, R. Easther, F. Finelli, R. Flauger, M. P. Hertzberg, K. Jones-Smith, S. Kachru, K. Kadota, J. Khoury, W. H. Kinney, E. Komatsu, L. M. Krauss, J. Lesgourgues, A. Liddle, M. Liguori, E. Lim, A. Linde, S. Matarrese, H. Mathur, L. McAllister, A. Melchiorri, A. Nicolis, L. Pagano, H. V. Peiris, M. Peloso, L. Pogosian, E. Pierpaoli, A. Riotto, U. Seljak, L. Senatore, S. Shandera, E. Silverstein, T. Smith, P. Vaudrevange, L. Verde, B. Wandelt, D. Wands, S. Watson, M. Wyman, A. Yadav, W. Valkenburg, and M. Zaldarriaga, *Probing Inflation with CMB Polarization*, in *American Institute of Physics Conference Series* (S. Dodelson, D. Baumann, A. Cooray, J. Dunkley, A. Fraisse, M. G. Jackson, A. Kogut, L. Krauss, M. Zaldarriaga, and K. Smith, eds.), vol. 1141 of *American Institute of Physics Conference Series*, pp. 10–120, June, 2009. [arXiv:0811.3919](#).
- [12] C. Carbone, C. Fedeli, L. Moscardini, and A. Cimatti, *Measuring the neutrino mass from future wide galaxy cluster catalogues*, *J. Cosmol. Astropart. Phys.* **3** (Mar., 2012) 23, [[arXiv:1112.4810](#)].
- [13] W. Hu, D. J. Eisenstein, and M. Tegmark, *Weighing Neutrinos with Galaxy Surveys*, *Physical Review Letters* **80** (June, 1998) 5255–5258, [[astro-ph/](#)].
- [14] Ø. Elgarøy, O. Lahav, W. J. Percival, J. A. Peacock, D. S. Madgwick, S. L. Bridle, C. M. Baugh, I. K. Baldry, J. Bland-Hawthorn, T. Bridges, R. Cannon, S. Cole, M. Colless, C. Collins, W. Couch, G. Dalton, R. de Propris, S. P. Driver, G. P. Efstathiou, R. S. Ellis, C. S. Frenk, K. Glazebrook, C. Jackson, I. Lewis, S. Lumsden, S. Maddox, P. Norberg, B. A. Peterson, W. Sutherland, and K. Taylor, *New Upper Limit on the Total Neutrino Mass from the 2 Degree Field Galaxy Redshift Survey*, *Physical Review Letters* **89** (July, 2002) 061301, [[astro-ph/](#)].
- [15] S. Hannestad, *Neutrino masses and the number of neutrino species from WMAP and 2dFGRS*, *J. Cosmol. Astropart. Phys.* **5** (May, 2003) 4, [[astro-ph/](#)].
- [16] S. W. Allen, R. W. Schmidt, and S. L. Bridle, *A preference for a non-zero neutrino mass from cosmological data*, *Mon. Not. R. Astron. Soc.* **346** (Dec., 2003) 593–600, [[astro-ph/](#)].
- [17] S. Hannestad and G. Raffelt, *Cosmological mass limits on neutrinos, axions, and other light particles*, *J. Cosmol. Astropart. Phys.* **4** (Apr., 2004) 8, [[hep-ph/03](#)].
- [18] V. Barger, D. Marfatia, and A. Tregre, *Neutrino mass limits from SDSS, 2dFGRS and WMAP*, *Physics Letters B* **595** (Aug., 2004) 55–59, [[hep-ph/03](#)].
- [19] P. Crotty, J. Lesgourgues, and S. Pastor, *Current cosmological bounds on neutrino masses and relativistic relics*, *Phys. Rev. D* **69** (June, 2004) 123007, [[hep-ph/04](#)].
- [20] M. Tegmark, M. A. Strauss, M. R. Blanton, K. Abazajian, S. Dodelson, H. Sandvik, X. Wang, D. H. Weinberg, I. Zehavi, N. A. Bahcall, F. Hoyle, D. Schlegel, R. Scoccimarro, M. S. Vogeley, A. Berlind, T. Budavari, A. Connolly, D. J. Eisenstein, D. Finkbeiner, J. A. Frieman, J. E. Gunn, L. Hui, B. Jain, D. Johnston, S. Kent, H. Lin, R. Nakajima, R. C. Nichol, J. P. Ostriker, A. Pope, R. Scranton, U. Seljak, R. K. Sheth, A. Stebbins, A. S. Szalay, I. Szapudi, Y. Xu, J. Annis, J. Brinkmann, S. Burles, F. J. Castander, I. Csabai, J. Loveday, M. Doi, M. Fukugita, B. Gillespie, G. Hennessy, D. W. Hogg, Ž. Ivezić, G. R. Knapp, D. Q. Lamb, B. C. Lee, R. H. Lupton, T. A. McKay, P. Kunszt, J. A. Munn, L. O’Connell, J. Peoples, J. R. Pier, M. Richmond, C. Rockosi, D. P. Schneider, C. Stoughton, D. L. Tucker, D. E. vanden Berk, B. Yanny, and D. G. York, *Cosmological parameters from SDSS and WMAP*, *Phys. Rev. D* **69** (May, 2004) 103501, [[astro-ph/](#)].
- [21] U. Seljak, A. Makarov, P. McDonald, S. F. Anderson, N. A. Bahcall, J. Brinkmann, S. Burles, R. Cen, M. Doi, J. E. Gunn, Ž. Ivezić, S. Kent, J. Loveday, R. H. Lupton, J. A. Munn, R. C. Nichol, J. P. Ostriker, D. J. Schlegel, D. P. Schneider, M. Tegmark, D. E. Berk, D. H. Weinberg, and D. G. York, *Cosmological parameter analysis including SDSS Ly α forest and galaxy bias: Constraints on the primordial spectrum of fluctuations, neutrino mass, and dark energy*, *Phys. Rev. D* **71** (May, 2005) 103515, [[astro-ph/](#)].

- [22] U. Seljak, A. Slosar, and P. McDonald, *Cosmological parameters from combining the Lyman- α forest with CMB, galaxy clustering and SN constraints*, *J. Cosmol. Astropart. Phys.* **10** (Oct., 2006) 14, [[astro-ph/](#)].
- [23] A. Goobar, S. Hannestad, E. Mörtzell, and H. Tu, *The neutrino mass bound from WMAP 3 year data, the baryon acoustic peak, the SNLS supernovae and the Lyman- α forest*, *J. Cosmol. Astropart. Phys.* **6** (June, 2006) 19, [[astro-ph/](#)].
- [24] G.-B. Zhao, J.-Q. Xia, and X. Zhang, *Probing for variation of neutrino mass with current observations*, *J. Cosmol. Astropart. Phys.* **7** (July, 2007) 10, [[astro-ph/](#)].
- [25] G. L. Fogli, E. Lisi, A. Marrone, A. Melchiorri, A. Palazzo, A. M. Rotunno, P. Serra, J. Silk, and A. Slosar, *Observables sensitive to absolute neutrino masses. II*, *Phys. Rev. D* **78** (Aug., 2008) 033010, [[arXiv:0805.2517](#)].
- [26] J.-Q. Xia, H. Li, G.-B. Zhao, and X. Zhang, *Determining cosmological parameters with the latest observational data*, *Phys. Rev. D* **78** (Oct., 2008) 083524, [[arXiv:0807.3878](#)].
- [27] T. Sekiguchi, K. Ichikawa, T. Takahashi, and L. Greenhill, *Neutrino mass from cosmology: impact of high-accuracy measurement of the Hubble constant*, *J. Cosmol. Astropart. Phys.* **3** (Mar., 2010) 15, [[arXiv:0911.0976](#)].
- [28] B. A. Reid, W. J. Percival, D. J. Eisenstein, L. Verde, D. N. Spergel, R. A. Skibba, N. A. Bahcall, T. Budavari, J. A. Frieman, M. Fukugita, J. R. Gott, J. E. Gunn, Ž. Ivezić, G. R. Knapp, R. G. Kron, R. H. Lupton, T. A. McKay, A. Meiksin, R. C. Nichol, A. C. Pope, D. J. Schlegel, D. P. Schneider, C. Stoughton, M. A. Strauss, A. S. Szalay, M. Tegmark, M. S. Vogeley, D. H. Weinberg, D. G. York, and I. Zehavi, *Cosmological constraints from the clustering of the Sloan Digital Sky Survey DR7 luminous red galaxies*, *Mon. Not. R. Astron. Soc.* **404** (May, 2010) 60–85, [[arXiv:0907.1659](#)].
- [29] S. A. Thomas, F. B. Abdalla, and O. Lahav, *Upper Bound of 0.28 eV on Neutrino Masses from the Largest Photometric Redshift Survey*, *Physical Review Letters* **105** (July, 2010) 031301, [[arXiv:0911.5291](#)].
- [30] S. Saito, M. Takada, and A. Taruya, *Neutrino mass constraint from the Sloan Digital Sky Survey power spectrum of luminous red galaxies and perturbation theory*, *Phys. Rev. D* **83** (Feb., 2011) 043529, [[arXiv:1006.4845](#)].
- [31] S. Riemer-Sørensen, C. Blake, D. Parkinson, T. M. Davis, S. Brough, M. Colless, C. Contreras, W. Couch, S. Croom, D. Croton, M. J. Drinkwater, K. Forster, D. Gilbank, M. Gladders, K. Glazebrook, B. Jelliffe, R. J. Jurek, I.-h. Li, B. Madore, D. C. Martin, K. Pimblet, G. B. Poole, M. Pracy, R. Sharp, E. Wisnioski, D. Woods, T. K. Wyder, and H. K. C. Yee, *WiggleZ Dark Energy Survey: Cosmological neutrino mass constraint from blue high-redshift galaxies*, *Phys. Rev. D* **85** (Apr., 2012) 081101, [[arXiv:1112.4940](#)].
- [32] J.-Q. Xia, B. R. Granett, M. Viel, S. Bird, L. Guzzo, M. G. Haehnelt, J. Coupon, H. J. McCracken, and Y. Mellier, *Constraints on massive neutrinos from the CFHTLS angular power spectrum*, *J. Cosmol. Astropart. Phys.* **6** (June, 2012) 10, [[arXiv:1203.5105](#)].
- [33] R. de Putter, O. Mena, E. Giusarma, S. Ho, A. Cuesta, H.-J. Seo, A. Ross, M. White, D. Bizyaev, H. Brewington, D. Kirkby, E. Malanushenko, V. Malanushenko, D. Oravetz, K. Pan, W. J. Percival, N. P. Ross, D. P. Schneider, A. Shelden, A. Simmons, and S. Snedden, *New Neutrino Mass Bounds from Sloan Digital Sky Survey III Data Release 8 Photometric Luminous Galaxies*, *ArXiv e-prints* (Jan., 2012) [[arXiv:1201.1909](#)].
- [34] D. M. Wittman, J. A. Tyson, D. Kirkman, I. Dell’Antonio, and G. Bernstein, *Detection of weak gravitational lensing distortions of distant galaxies by cosmic dark matter at large scales*, *Nature* **405** (May, 2000) 143–148, [[astro-ph/](#)].
- [35] D. J. Bacon, A. R. Refregier, and R. S. Ellis, *Detection of weak gravitational lensing by large-scale structure*, *Mon. Not. R. Astron. Soc.* **318** (Oct., 2000) 625–640, [[astro-ph/](#)].

- [36] L. Van Waerbeke, Y. Mellier, T. Erben, J. C. Cuillandre, F. Bernardeau, R. Maoli, E. Bertin, H. J. McCracken, O. Le Fèvre, B. Fort, M. Dantel-Fort, B. Jain, and P. Schneider, *Detection of correlated galaxy ellipticities from CFHT data: first evidence for gravitational lensing by large-scale structures*, *A&A* **358** (June, 2000) 30–44, [[astro-ph/](#)].
- [37] N. Kaiser, G. Wilson, and G. A. Luppino, *Large-Scale Cosmic Shear Measurements*, *ArXiv Astrophysics e-prints* (Mar., 2000) [[astro-ph/](#)].
- [38] M. Bartelmann and P. Schneider, *Weak gravitational lensing*, *Phys. Rept.* **340** (Jan., 2001) 291–472, [[astro-ph/](#)].
- [39] D. Huterer, *Weak lensing, dark matter and dark energy*, *General Relativity and Gravitation* **42** (Sept., 2010) 2177–2195, [[arXiv:1001.1758](#)].
- [40] A. R. Cooray, *Weighing neutrinos: weak lensing approach*, *A&A* **348** (Aug., 1999) 31–37, [[astro-ph/](#)].
- [41] K. Abazajian and S. Dodelson, *Neutrino Mass and Dark Energy from Weak Lensing*, *Physical Review Letters* **91** (July, 2003) 041301, [[astro-ph/](#)].
- [42] S. Hannestad, H. Tu, and Y. Y. Wong, *Measuring neutrino masses and dark energy with weak lensing tomography*, *J. Cosmol. Astropart. Phys.* **6** (June, 2006) 25, [[astro-ph/](#)].
- [43] S. Joudaki and M. Kaplinghat, *Dark energy and neutrino masses from future measurements of the expansion history and growth of structure*, *Phys. Rev. D* **86** (July, 2012) 023526, [[arXiv:1106.0299](#)].
- [44] H. Li, J. Liu, J.-Q. Xia, L. Sun, Z.-H. Fan, C. Tao, A. Tilquin, and X. Zhang, *Constraining cosmological parameters with observational data including weak lensing effects*, *Physics Letters B* **675** (May, 2009) 164–169, [[arXiv:0812.1672](#)].
- [45] I. Tereno, C. Schimd, J.-P. Uzan, M. Kilbinger, F. H. Vincent, and L. Fu, *CFHTLS weak-lensing constraints on the neutrino masses*, *A&A* **500** (June, 2009) 657–665, [[arXiv:0810.0555](#)].
- [46] K. Ichiki, M. Takada, and T. Takahashi, *Constraints on neutrino masses from weak lensing*, *Phys. Rev. D* **79** (Jan., 2009) 023520, [[arXiv:0810.4921](#)].
- [47] Z.-L. Yi and T.-J. Zhang, *Constraints on Holographic Dark Energy Models Using the Differential Ages of Passively Evolving Galaxies*, *Modern Physics Letters A* **22** (2007) 41–53, [[astro-ph/](#)].
- [48] T.-J. Zhang, C. Ma, and T. Lan, *Constraints on the Dark Side of the Universe and Observational Hubble Parameter Data*, *Advances in Astronomy* **2010** (2010) [[arXiv:1010.1307](#)].
- [49] R. Jimenez and A. Loeb, *Constraining Cosmological Parameters Based on Relative Galaxy Ages*, *Astrophys. J.* **573** (July, 2002) 37–42, [[astro-ph/](#)].
- [50] D. Stern, R. Jimenez, L. Verde, M. Kamionkowski, and S. A. Stanford, *Cosmic chronometers: constraining the equation of state of dark energy. I: $H(z)$ measurements*, *J. Cosmol. Astropart. Phys.* **2** (Feb., 2010) 8, [[arXiv:0907.3149](#)].
- [51] M. Moresco, L. Verde, L. Pozzetti, R. Jimenez, and A. Cimatti, *New constraints on cosmological parameters and neutrino properties using the expansion rate of the Universe to $z \sim 1.75$* , *J. Cosmol. Astropart. Phys.* **7** (July, 2012) 53, [[arXiv:1201.6658](#)].
- [52] S. Hannestad, *Neutrino Masses and the Dark Energy Equation of State: Relaxing the Cosmological Neutrino Mass Bound*, *Physical Review Letters* **95** (Nov., 2005) 221301, [[astro-ph/](#)].
- [53] S. Hannestad and G. G. Raffelt, *Neutrino masses and cosmic radiation density: combined analysis*, *J. Cosmol. Astropart. Phys.* **11** (Nov., 2006) 16, [[astro-ph/](#)].
- [54] J. Hamann, S. Hannestad, G. G. Raffelt, and Y. Y. Y. Wong, *Observational bounds on the cosmic radiation density*, *J. Cosmol. Astropart. Phys.* **8** (Aug., 2007) 21, [[arXiv:0705.0440](#)].
- [55] J. Hamann, S. Hannestad, G. G. Raffelt, I. Tamborra, and Y. Y. Y. Wong, *Cosmology Favoring Extra Radiation and Sub-eV Mass Sterile Neutrinos as an Option*, *Physical Review Letters* **105** (Oct., 2010) 181301, [[arXiv:1006.5276](#)].

- [56] G. Mangano, G. Miele, S. Pastor, T. Pinto, O. Pisanti, and P. D. Serpico, *Relic neutrino decoupling including flavour oscillations*, *Nuclear Physics B* **729** (Nov., 2005) 221–234, [[hep-ph/05](#)].
- [57] D. A. Dicus, E. W. Kolb, A. M. Gleeson, E. C. G. Sudarshan, V. L. Teplitz, and M. S. Turner, *Primordial nucleosynthesis including radiative, Coulomb, and finite-temperature corrections to weak rates*, *Phys. Rev. D* **26** (Nov., 1982) 2694–2706.
- [58] A. F. Heckler, *Astrophysical applications of quantum corrections to the equation of state of a plasma*, *Phys. Rev. D* **49** (Jan., 1994) 611–617.
- [59] A. D. Dolgov, S. H. Hansen, S. Pastor, S. T. Petcov, G. G. Raffelt, and D. V. Semikoz, *Cosmological bounds on neutrino degeneracy improved by flavor oscillations*, *Nuclear Physics B* **632** (June, 2002) 363–382, [[hep-ph/02](#)].
- [60] D. N. Spergel, R. Bean, O. Doré, M. R. Nolta, C. L. Bennett, J. Dunkley, G. Hinshaw, N. Jarosik, E. Komatsu, L. Page, H. V. Peiris, L. Verde, M. Halpern, R. S. Hill, A. Kogut, M. Limon, S. S. Meyer, N. Odegard, G. S. Tucker, J. L. Weiland, E. Wollack, and E. L. Wright, *Three-Year Wilkinson Microwave Anisotropy Probe (WMAP) Observations: Implications for Cosmology*, *Astrophys. J. Suppl.* **170** (June, 2007) 377–408, [[astro-ph/](#)].
- [61] J. Dunkley, E. Komatsu, M. R. Nolta, D. N. Spergel, D. Larson, G. Hinshaw, L. Page, C. L. Bennett, B. Gold, N. Jarosik, J. L. Weiland, M. Halpern, R. S. Hill, A. Kogut, M. Limon, S. S. Meyer, G. S. Tucker, E. Wollack, and E. L. Wright, *Five-Year Wilkinson Microwave Anisotropy Probe Observations: Likelihoods and Parameters from the WMAP Data*, *Astrophys. J. Suppl.* **180** (Feb., 2009) 306–329, [[arXiv:0803.0586](#)].
- [62] J. Dunkley, R. Hlozek, J. Sievers, V. Acquaviva, P. A. R. Ade, P. Aguirre, M. Amiri, J. W. Appel, L. F. Barrientos, E. S. Battistelli, J. R. Bond, B. Brown, B. Burger, J. Chervenak, S. Das, M. J. Devlin, S. R. Dicker, W. Bertrand Doriese, R. Dünner, T. Essinger-Hileman, R. P. Fisher, J. W. Fowler, A. Hajian, M. Halpern, M. Hasselfield, C. Hernández-Monteagudo, G. C. Hilton, M. Hilton, A. D. Hincks, K. M. Huffenberger, D. H. Hughes, J. P. Hughes, L. Infante, K. D. Irwin, J. B. Juin, M. Kaul, J. Klein, A. Kosowsky, J. M. Lau, M. Limon, Y.-T. Lin, R. H. Lupton, T. A. Marriage, D. Marsden, P. Mauskopf, F. Menanteau, K. Moodley, H. Moseley, C. B. Netterfield, M. D. Niemack, M. R. Nolta, L. A. Page, L. Parker, B. Partridge, B. Reid, N. Sehgal, B. Sherwin, D. N. Spergel, S. T. Staggs, D. S. Swetz, E. R. Switzer, R. Thornton, H. Trac, C. Tucker, R. Warne, E. Wollack, and Y. Zhao, *The Atacama Cosmology Telescope: Cosmological Parameters from the 2008 Power Spectrum*, *Astrophys. J.* **739** (Sept., 2011) 52, [[arXiv:1009.0866](#)].
- [63] R. Keisler, C. L. Reichardt, K. A. Aird, B. A. Benson, L. E. Bleem, J. E. Carlstrom, C. L. Chang, H. M. Cho, T. M. Crawford, A. T. Crites, T. de Haan, M. A. Dobbs, J. Dudley, E. M. George, N. W. Halverson, G. P. Holder, W. L. Holzzapfel, S. Hoover, Z. Hou, J. D. Hrubes, M. Joy, L. Knox, A. T. Lee, E. M. Leitch, M. Lueker, D. Luong-Van, J. J. McMahon, J. Mehl, S. S. Meyer, M. Millea, J. J. Mohr, T. E. Montroy, T. Natoli, S. Padin, T. Plagge, C. Pryke, J. E. Ruhl, K. K. Schaffer, L. Shaw, E. Shirokoff, H. G. Spieler, Z. Staniszewski, A. A. Stark, K. Story, A. van Engelen, K. Vanderlinde, J. D. Vieira, R. Williamson, and O. Zahn, *A Measurement of the Damping Tail of the Cosmic Microwave Background Power Spectrum with the South Pole Telescope*, *Astrophys. J.* **743** (Dec., 2011) 28, [[arXiv:1105.3182](#)].
- [64] K. Ichikawa, M. Kawasaki, K. Nakayama, M. Senami, and F. Takahashi, *Increasing the effective number of neutrinos with decaying particles*, *J. Cosmol. Astropart. Phys.* **5** (May, 2007) 8, [[hep-ph/07](#)].
- [65] M. Archidiacono, E. Calabrese, and A. Melchiorri, *Case for dark radiation*, *Phys. Rev. D* **84** (Dec., 2011) 123008, [[arXiv:1109.2767](#)].
- [66] M. Archidiacono, E. Giusarma, A. Melchiorri, and O. Mena, *Dark Radiation in extended cosmological scenarios*, *ArXiv e-prints* (June, 2012) [[arXiv:1206.0109](#)].
- [67] S. Joudaki, *Constraints on Neutrino Mass and Light Degrees of Freedom in Extended Cosmological Parameter Spaces*, *ArXiv e-prints* (Jan., 2012) [[arXiv:1202.0005](#)].

- [68] D. Huterer, *Weak lensing and dark energy*, Phys. Rev. D **65** (Mar., 2002) 063001, [[astro-ph/](#)].
- [69] W. Hu, *Dark Energy Probes in Light of the CMB*, in *Observing Dark Energy* (S. C. Wolff and T. R. Lauer, eds.), vol. 339 of *Astronomical Society of the Pacific Conference Series*, p. 215, Aug., 2005. [[astro-ph/](#)].
- [70] E. Komatsu, J. Dunkley, M. R. Nolta, C. L. Bennett, B. Gold, G. Hinshaw, N. Jarosik, D. Larson, M. Limon, L. Page, D. N. Spergel, M. Halpern, R. S. Hill, A. Kogut, S. S. Meyer, G. S. Tucker, J. L. Weiland, E. Wollack, and E. L. Wright, *Five-Year Wilkinson Microwave Anisotropy Probe Observations: Cosmological Interpretation*, Astrophys. J. Suppl. **180** (Feb., 2009) 330–376, [[arXiv:0803.0547](#)].
- [71] J. M. Bardeen, J. R. Bond, N. Kaiser, and A. S. Szalay, *The statistics of peaks of Gaussian random fields*, Astrophys. J. **304** (May, 1986) 15–61.
- [72] C.-P. Ma and E. Bertschinger, *Cosmological Perturbation Theory in the Synchronous and Conformal Newtonian Gauges*, Astrophys. J. **455** (Dec., 1995) 7, [[astro-ph/](#)].
- [73] D. J. Eisenstein and W. Hu, *Baryonic Features in the Matter Transfer Function*, Astrophys. J. **496** (Mar., 1998) 605, [[astro-ph/](#)].
- [74] S. Agarwal and H. A. Feldman, *The effect of massive neutrinos on the matter power spectrum*, Mon. Not. R. Astron. Soc. **410** (Jan., 2011) 1647–1654, [[arXiv:1006.0689](#)].
- [75] Y. Y. Y. Wong, *Higher order corrections to the large scale matter power spectrum in the presence of massive neutrinos*, J. Cosmol. Astropart. Phys. **10** (Oct., 2008) 35, [[arXiv:0809.0693](#)].
- [76] S. Saito, M. Takada, and A. Taruya, *Impact of Massive Neutrinos on the Nonlinear Matter Power Spectrum*, Physical Review Letters **100** (May, 2008) 191301, [[arXiv:0801.0607](#)].
- [77] S. Saito, M. Takada, and A. Taruya, *Nonlinear power spectrum in the presence of massive neutrinos: Perturbation theory approach, galaxy bias, and parameter forecasts*, Phys. Rev. D **80** (Oct., 2009) 083528, [[arXiv:0907.2922](#)].
- [78] J. Lesgourgues, S. Matarrese, M. Pietroni, and A. Riotto, *Non-linear power spectrum including massive neutrinos: the time-RG flow approach*, J. Cosmol. Astropart. Phys. **6** (June, 2009) 17, [[arXiv:0901.4550](#)].
- [79] R. E. Smith, J. A. Peacock, A. Jenkins, S. D. M. White, C. S. Frenk, F. R. Pearce, P. A. Thomas, G. Efstathiou, and H. M. P. Couchman, *Stable clustering, the halo model and non-linear cosmological power spectra*, Mon. Not. R. Astron. Soc. **341** (June, 2003) 1311–1332, [[astro-ph/](#)].
- [80] S. Bird, M. Viel, and M. G. Haehnelt, *Massive neutrinos and the non-linear matter power spectrum*, Mon. Not. R. Astron. Soc. **420** (Mar., 2012) 2551–2561, [[arXiv:1109.4416](#)].
- [81] D. Munshi, P. Valageas, L. van Waerbeke, and A. Heavens, *Cosmology with weak lensing surveys*, Phys. Rept. **462** (June, 2008) 67–121, [[astro-ph/](#)].
- [82] L. Fu, E. Semboloni, H. Hoekstra, M. Kilbinger, L. van Waerbeke, I. Tereno, Y. Mellier, C. Heymans, J. Coupon, K. Benabed, J. Benjamin, E. Bertin, O. Doré, M. J. Hudson, O. Ilbert, R. Maoli, C. Marmo, H. J. McCracken, and B. Ménard, *Very weak lensing in the CFHTLS wide: cosmology from cosmic shear in the linear regime*, A&A **479** (Feb., 2008) 9–25, [[arXiv:0712.0884](#)].
- [83] M. Kilbinger, K. Benabed, J. Guy, P. Astier, I. Tereno, L. Fu, D. Wraith, J. Coupon, Y. Mellier, C. Bland, F. R. Bouchet, T. Hamana, D. Hardin, H. J. McCracken, R. Pain, N. Regnault, M. Schultheis, and H. Yahagi, *Dark-energy constraints and correlations with systematics from CFHTLS weak lensing, SNLS supernovae Ia and WMAP5*, A&A **497** (Apr., 2009) 677–688, [[arXiv:0810.5129](#)].
- [84] P. Schneider, L. van Waerbeke, B. Jain, and G. Kruse, *A new measure for cosmic shear*, Mon. Not. R. Astron. Soc. **296** (June, 1998) 873–892, [[astro-ph/](#)].

- [85] P. Schneider, L. van Waerbeke, M. Kilbinger, and Y. Mellier, *Analysis of two-point statistics of cosmic shear. I. Estimators and covariances*, *A&A* **396** (Dec., 2002) 1–19, [[astro-ph/](#)].
- [86] N. Suzuki, D. Rubin, C. Lidman, G. Aldering, R. Amanullah, K. Barbary, L. F. Barrientos, J. Botyanszki, M. Brodwin, N. Connolly, K. S. Dawson, A. Dey, M. Doi, M. Donahue, S. Deustua, P. Eisenhardt, E. Ellingson, L. Faccioli, V. Fadeyev, H. K. Fakhouri, A. S. Fruchter, D. G. Gilbank, M. D. Gladders, G. Goldhaber, A. H. Gonzalez, A. Goobar, A. Gude, T. Hattori, H. Hoekstra, E. Hsiao, X. Huang, Y. Ihara, M. J. Jee, D. Johnston, N. Kashikawa, B. Koester, K. Konishi, M. Kowalski, E. V. Linder, L. Lubin, J. Melbourne, J. Meyers, T. Morokuma, F. Munshi, C. Mullis, T. Oda, N. Panagia, S. Perlmutter, M. Postman, T. Pritchard, J. Rhodes, P. Ripoche, P. Rosati, D. J. Schlegel, A. Spadafora, S. A. Stanford, V. Stanishev, D. Stern, M. Strovink, N. Takanashi, K. Tokita, M. Wagner, L. Wang, N. Yasuda, H. K. C. Yee, and T. Supernova Cosmology Project, *The Hubble Space Telescope Cluster Supernova Survey. V. Improving the Dark-energy Constraints above $z > 1$ and Building an Early-type-hosted Supernova Sample*, *Astrophys. J.* **746** (Feb., 2012) 85, [[arXiv:1105.3470](#)].
- [87] R. Amanullah, C. Lidman, D. Rubin, G. Aldering, P. Astier, K. Barbary, M. S. Burns, A. Conley, K. S. Dawson, S. E. Deustua, M. Doi, S. Fabbro, L. Faccioli, H. K. Fakhouri, G. Folatelli, A. S. Fruchter, H. Furusawa, G. Garavini, G. Goldhaber, A. Goobar, D. E. Groom, I. Hook, D. A. Howell, N. Kashikawa, A. G. Kim, R. A. Knop, M. Kowalski, E. Linder, J. Meyers, T. Morokuma, S. Nobili, J. Nordin, P. E. Nugent, L. Östman, R. Pain, N. Panagia, S. Perlmutter, J. Raux, P. Ruiz-Lapuente, A. L. Spadafora, M. Strovink, N. Suzuki, L. Wang, W. M. Wood-Vasey, N. Yasuda, and T. Supernova Cosmology Project, *Spectra and Hubble Space Telescope Light Curves of Six Type Ia Supernovae at $0.511 < z < 1.12$ and the Union2 Compilation*, *Astrophys. J.* **716** (June, 2010) 712–738, [[arXiv:1004.1711](#)].
- [88] W. M. Wood-Vasey, G. Miknaitis, C. W. Stubbs, S. Jha, A. G. Riess, P. M. Garnavich, R. P. Kirshner, C. Aguilera, A. C. Becker, J. W. Blackman, S. Blondin, P. Challis, A. Clocchiatti, A. Conley, R. Covarrubias, T. M. Davis, A. V. Filippenko, R. J. Foley, A. Garg, M. Hicken, K. Krisciunas, B. Leibundgut, W. Li, T. Matheson, A. Miceli, G. Narayan, G. Pignata, J. L. Prieto, A. Rest, M. E. Salvo, B. P. Schmidt, R. C. Smith, J. Sollerman, J. Spyromilio, J. L. Tonry, N. B. Suntzeff, and A. Zenteno, *Observational Constraints on the Nature of Dark Energy: First Cosmological Results from the ESSENCE Supernova Survey*, *Astrophys. J.* **666** (Sept., 2007) 694–715, [[astro-ph/](#)].
- [89] M. Hicken, W. M. Wood-Vasey, S. Blondin, P. Challis, S. Jha, P. L. Kelly, A. Rest, and R. P. Kirshner, *Improved Dark Energy Constraints from ~ 100 New CfA Supernova Type Ia Light Curves*, *Astrophys. J.* **700** (Aug., 2009) 1097–1140, [[arXiv:0901.4804](#)].
- [90] R. Kessler, A. C. Becker, D. Cinabro, J. Vanderplas, J. A. Frieman, J. Murrin, T. M. Davis, B. Dilday, J. Holtzman, S. W. Jha, H. Lampeitl, M. Sako, M. Smith, C. Zheng, R. C. Nichol, B. Bassett, R. Bender, D. L. Depoy, M. Doi, E. Elson, A. V. Filippenko, R. J. Foley, P. M. Garnavich, U. Hopp, Y. Ihara, W. Ketzeback, W. Kollatschny, K. Konishi, J. L. Marshall, R. J. McMillan, G. Miknaitis, T. Morokuma, E. Mörtzell, K. Pan, J. L. Prieto, M. W. Richmond, A. G. Riess, R. Romani, D. P. Schneider, J. Sollerman, N. Takanashi, K. Tokita, K. van der Heyden, J. C. Wheeler, N. Yasuda, and D. York, *First-Year Sloan Digital Sky Survey-II Supernova Results: Hubble Diagram and Cosmological Parameters*, *Astrophys. J. Suppl.* **185** (Nov., 2009) 32–84, [[arXiv:0908.4274](#)].
- [91] A. Conley, J. Guy, M. Sullivan, N. Regnault, P. Astier, C. Balland, S. Basa, R. G. Carlberg, D. Fouchez, D. Hardin, I. M. Hook, D. A. Howell, R. Pain, N. Palanque-Delabrouille, K. M. Perrett, C. J. Pritchard, J. Rich, V. Ruhlmann-Kleider, D. Balam, S. Baumont, R. S. Ellis, S. Fabbro, H. K. Fakhouri, N. Fourmanoit, S. González-Gaitán, M. L. Graham, M. J. Hudson, E. Hsiao, T. Kronborg, C. Lidman, A. M. Mourao, J. D. Neill, S. Perlmutter, P. Ripoche, N. Suzuki, and E. S. Walker, *Supernova Constraints and Systematic Uncertainties from the First Three Years of the Supernova Legacy Survey*, *Astrophys. J. Suppl.* **192** (Jan., 2011) 1, [[arXiv:1104.1443](#)].
- [92] J. Guy, P. Astier, S. Baumont, D. Hardin, R. Pain, N. Regnault, S. Basa, R. G. Carlberg, A. Conley, S. Fabbro, D. Fouchez, I. M. Hook, D. A. Howell, K. Perrett, C. J. Pritchard, J. Rich, M. Sullivan, P. Antilogus, E. Aubourg, G. Bazin, J. Bronder, M. Filiol, N. Palanque-Delabrouille, P. Ripoche, and

- V. Ruhlmann-Kleider, *SALT2: using distant supernovae to improve the use of type Ia supernovae as distance indicators*, *A&A* **466** (Apr., 2007) 11–21, [[astro-ph/](#)].
- [93] S. Jha, A. G. Riess, and R. P. Kirshner, *Improved Distances to Type Ia Supernovae with Multicolor Light-Curve Shapes: MLCS2k2*, *Astrophys. J.* **659** (Apr., 2007) 122–148, [[astro-ph/](#)].
- [94] A. Conley, M. Sullivan, E. Y. Hsiao, J. Guy, P. Astier, D. Balam, C. Balland, S. Basa, R. G. Carlberg, D. Fouchez, D. Hardin, D. A. Howell, I. M. Hook, R. Pain, K. Perrett, C. J. Pritchett, and N. Regnault, *SiFTO: An Empirical Method for Fitting SN Ia Light Curves*, *Astrophys. J.* **681** (July, 2008) 482–498, [[arXiv:0803.3441](#)].
- [95] G. R. Bengochea, *Supernova light-curve fitters and dark energy*, *Physics Letters B* **696** (Jan., 2011) 5–12, [[arXiv:1010.4014](#)].
- [96] Z. Li, P. Wu, and H. Yu, *Testing Nonstandard Cosmological Models with SNLS3 Supernova Data and Other Cosmological Probes*, *Astrophys. J.* **744** (Jan., 2012) 176, [[arXiv:1109.6125](#)].
- [97] P. J. E. Peebles and J. T. Yu, *Primeval Adiabatic Perturbation in an Expanding Universe*, *Astrophys. J.* **162** (Dec., 1970) 815.
- [98] W. Hu and N. Sugiyama, *Small-Scale Cosmological Perturbations: an Analytic Approach*, *Astrophys. J.* **471** (Nov., 1996) 542, [[astro-ph/](#)].
- [99] D. J. Eisenstein, I. Zehavi, D. W. Hogg, R. Scoccimarro, M. R. Blanton, R. C. Nichol, R. Scranton, H.-J. Seo, M. Tegmark, Z. Zheng, S. F. Anderson, J. Annis, N. Bahcall, J. Brinkmann, S. Burles, F. J. Castander, A. Connolly, I. Csabai, M. Doi, M. Fukugita, J. A. Frieman, K. Glazebrook, J. E. Gunn, J. S. Hendry, G. Hennessy, Z. Ivezić, S. Kent, G. R. Knapp, H. Lin, Y.-S. Loh, R. H. Lupton, B. Margon, T. A. McKay, A. Meiksin, J. A. Munn, A. Pope, M. W. Richmond, D. Schlegel, D. P. Schneider, K. Shimasaku, C. Stoughton, M. A. Strauss, M. SubbaRao, A. S. Szalay, I. Szapudi, D. L. Tucker, B. Yanny, and D. G. York, *Detection of the Baryon Acoustic Peak in the Large-Scale Correlation Function of SDSS Luminous Red Galaxies*, *Astrophys. J.* **633** (Nov., 2005) 560–574, [[astro-ph/](#)].
- [100] W. J. Percival, B. A. Reid, D. J. Eisenstein, N. A. Bahcall, T. Budavari, J. A. Frieman, M. Fukugita, J. E. Gunn, Ž. Ivezić, G. R. Knapp, R. G. Kron, J. Loveday, R. H. Lupton, T. A. McKay, A. Meiksin, R. C. Nichol, A. C. Pope, D. J. Schlegel, D. P. Schneider, D. N. Spergel, C. Stoughton, M. A. Strauss, A. S. Szalay, M. Tegmark, M. S. Vogeley, D. H. Weinberg, D. G. York, and I. Zehavi, *Baryon acoustic oscillations in the Sloan Digital Sky Survey Data Release 7 galaxy sample*, *Mon. Not. R. Astron. Soc.* **401** (Feb., 2010) 2148–2168, [[arXiv:0907.1660](#)].
- [101] C. Blake, E. A. Kazin, F. Beutler, T. M. Davis, D. Parkinson, S. Brough, M. Colless, C. Contreras, W. Couch, S. Croom, D. Croton, M. J. Drinkwater, K. Forster, D. Gilbank, M. Gladders, K. Glazebrook, B. Jelliffe, R. J. Jurek, I.-H. Li, B. Madore, D. C. Martin, K. Pimbblet, G. B. Poole, M. Pracy, R. Sharp, E. Wisnioski, D. Woods, T. K. Wyder, and H. K. C. Yee, *The WiggleZ Dark Energy Survey: mapping the distance-redshift relation with baryon acoustic oscillations*, *Mon. Not. R. Astron. Soc.* **418** (Dec., 2011) 1707–1724, [[arXiv:1108.2635](#)].
- [102] A. G. Riess, L. Macri, S. Casertano, M. Sosey, H. Lampeitl, H. C. Ferguson, A. V. Filippenko, S. W. Jha, W. Li, R. Chornock, and D. Sarkar, *A Redetermination of the Hubble Constant with the Hubble Space Telescope from a Differential Distance Ladder*, *Astrophys. J.* **699** (July, 2009) 539–563, [[arXiv:0905.0695](#)].
- [103] A. Smith, M. Archidiacono, A. Cooray, F. De Bernardis, A. Melchiorri, and J. Smidt, *Impact of assuming flatness in the determination of neutrino properties from cosmological data*, *Phys. Rev. D* **85** (June, 2012) 123521, [[arXiv:1112.3006](#)].
- [104] B. A. Reid, L. Verde, R. Jimenez, and O. Mena, *Robust neutrino constraints by combining low redshift observations with the CMB*, *J. Cosmol. Astropart. Phys.* **1** (Jan., 2010) 3, [[arXiv:0910.0008](#)].
- [105] A. Lewis and S. Bridle, *Cosmological parameters from CMB and other data: A Monte Carlo approach*, *Phys. Rev. D* **66** (Nov., 2002) 103511, [[astro-ph/](#)].

- [106] H. Lin, C. Hao, X. Wang, Q. Yuan, Z.-L. Yi, T.-J. Zhang, and B.-Q. Wang, *Observational $H(z)$ Data as a Complementarity to Other Cosmological Probes*, *Modern Physics Letters A* **24** (2009) 1699–1709, [[arXiv:0804.3135](#)].
- [107] C. Ma and T.-J. Zhang, *Power of Observational Hubble Parameter Data: A Figure of Merit Exploration*, *Astrophys. J.* **730** (Apr., 2011) 74, [[arXiv:1007.3787](#)].
- [108] C. L. Reichardt, B. Stalder, L. E. Bleem, T. E. Montroy, K. A. Aird, K. Andersson, R. Armstrong, M. L. N. Ashby, M. Bautz, M. Bayliss, G. Bazin, B. A. Benson, M. Brodwin, J. E. Carlstrom, C. L. Chang, H. M. Cho, A. Clocchiatti, T. M. Crawford, A. T. Crites, T. de Haan, S. Desai, M. A. Dobbs, J. P. Dudley, R. J. Foley, W. R. Forman, E. M. George, M. D. Gladders, A. H. Gonzalez, N. W. Halverson, N. L. Harrington, F. W. High, G. P. Holder, W. L. Holzapfel, S. Hoover, J. D. Hrubes, C. Jones, M. Joy, R. Keisler, L. Knox, A. T. Lee, E. M. Leitch, J. Liu, M. Lueker, D. Luong-Van, A. Mantz, D. P. Marrone, M. McDonald, J. J. McMahon, J. Mehl, S. S. Meyer, L. Mocuano, J. J. Mohr, S. S. Murray, T. Natoli, S. Padin, T. Plagge, C. Pryke, A. Rest, J. Ruel, J. E. Ruhl, B. R. Saliwanchik, A. Saro, J. T. Sayre, K. K. Schaffer, L. Shaw, E. Shirokoff, J. Song, H. G. Spieler, Z. Staniszewski, A. A. Stark, K. Story, C. W. Stubbs, R. Suhada, A. van Engelen, K. Vanderlinde, J. D. Vieira, A. Vikhlinin, R. Williamson, O. Zahn, and A. Zenteno, *Galaxy clusters discovered via the Sunyaev-Zel'dovich effect in the first 720 square degrees of the South Pole Telescope survey*, *ArXiv e-prints* (Mar., 2012) [[arXiv:1203.5775](#)].
- [109] A. Lewis, A. Challinor, and A. Lasenby, *Efficient Computation of Cosmic Microwave Background Anisotropies in Closed Friedmann-Robertson-Walker Models*, *Astrophys. J.* **538** (Aug., 2000) 473–476, [[astro-ph/](#)].
- [110] M. Takada, E. Komatsu, and T. Futamase, *Cosmology with high-redshift galaxy survey: Neutrino mass and inflation*, *Phys. Rev. D* **73** (Apr., 2006) 083520, [[astro-ph/](#)].
- [111] J. R. Bond, G. Efstathiou, and J. Silk, *Massive neutrinos and the large-scale structure of the universe*, *Physical Review Letters* **45** (Dec., 1980) 1980–1984.
- [112] M. Shoji and E. Komatsu, *Massive neutrinos in cosmology: Analytic solutions and fluid approximation*, *Phys. Rev. D* **81** (June, 2010) 123516.
- [113] J. Brandbyge, S. Hannestad, T. Haugbølle, and B. Thomsen, *The effect of thermal neutrino motion on the non-linear cosmological matter power spectrum*, *J. Cosmol. Astropart. Phys.* **8** (Aug., 2008) 20, [[arXiv:0802.3700](#)].
- [114] K. Ichikawa, T. Sekiguchi, and T. Takahashi, *Probing the effective number of neutrino species with the cosmic microwave background*, *Phys. Rev. D* **78** (Oct., 2008) 083526, [[arXiv:0803.0889](#)].
- [115] S. Bashinsky and U. Seljak, *Signatures of relativistic neutrinos in CMB anisotropy and matter clustering*, *Phys. Rev. D* **69** (Apr., 2004) 083002, [[astro-ph/](#)].
- [116] M. Tegmark, D. J. Eisenstein, M. A. Strauss, D. H. Weinberg, M. R. Blanton, J. A. Frieman, M. Fukugita, J. E. Gunn, A. J. S. Hamilton, G. R. Knapp, R. C. Nichol, J. P. Ostriker, N. Padmanabhan, W. J. Percival, D. J. Schlegel, D. P. Schneider, R. Scoccimarro, U. Seljak, H.-J. Seo, M. Swanson, A. S. Szalay, M. S. Vogeley, J. Yoo, I. Zehavi, K. Abazajian, S. F. Anderson, J. Annis, N. A. Bahcall, B. Bassett, A. Berlind, J. Brinkmann, T. Budavari, F. Castander, A. Connolly, I. Csabai, M. Doi, D. P. Finkbeiner, B. Gillespie, K. Glazebrook, G. S. Hennessy, D. W. Hogg, Ž. Ivezić, B. Jain, D. Johnston, S. Kent, D. Q. Lamb, B. C. Lee, H. Lin, J. Loveday, R. H. Lupton, J. A. Munn, K. Pan, C. Park, J. Peoples, J. R. Pier, A. Pope, M. Richmond, C. Rockosi, R. Scranton, R. K. Sheth, A. Stebbins, C. Stoughton, I. Szapudi, D. L. Tucker, D. E. vanden Berk, B. Yanny, and D. G. York, *Cosmological constraints from the SDSS luminous red galaxies*, *Phys. Rev. D* **74** (Dec., 2006) 123507, [[astro-ph/](#)].
- [117] K. Ichikawa, M. Fukugita, and M. Kawasaki, *Constraining neutrino masses by CMB experiments alone*, *Phys. Rev. D* **71** (Feb., 2005) 043001, [[astro-ph/](#)].
- [118] S. Joudaki, A. Cooray, and D. E. Holz, *Weak lensing and dark energy: The impact of dark energy on nonlinear dark matter clustering*, *Phys. Rev. D* **80** (July, 2009) 023003, [[arXiv:0904.4697](#)].

- [119] P. McDonald, H. Trac, and C. Contaldi, *Dependence of the non-linear mass power spectrum on the equation of state of dark energy*, Mon. Not. R. Astron. Soc. **366** (Feb., 2006) 547–556, [[astro-ph/](#)].
- [120] D. Huterer and M. Takada, *Calibrating the nonlinear matter power spectrum: Requirements for future weak lensing surveys*, *Astroparticle Physics* **23** (May, 2005) 369–376, [[astro-ph/](#)].
- [121] H. Zhan and L. Knox, *Effect of Hot Baryons on the Weak-Lensing Shear Power Spectrum*, *Astrophys. J.* **616** (Dec., 2004) L75–L78, [[astro-ph/](#)].
- [122] M. P. van Daalen, J. Schaye, C. M. Booth, and C. Dalla Vecchia, *The effects of galaxy formation on the matter power spectrum: a challenge for precision cosmology*, Mon. Not. R. Astron. Soc. **415** (Aug., 2011) 3649–3665, [[arXiv:1104.1174](#)].
- [123] E. Semboloni, H. Hoekstra, J. Schaye, M. P. van Daalen, and I. G. McCarthy, *Quantifying the effect of baryon physics on weak lensing tomography*, Mon. Not. R. Astron. Soc. **417** (Nov., 2011) 2020–2035, [[arXiv:1105.1075](#)].
- [124] D. Huterer, M. Takada, G. Bernstein, and B. Jain, *Systematic errors in future weak-lensing surveys: requirements and prospects for self-calibration*, Mon. Not. R. Astron. Soc. **366** (Feb., 2006) 101–114, [[astro-ph/](#)].
- [125] J. Hamann, S. Hannestad, and Y. Y. Y. Wong, *Measuring neutrino masses with a future galaxy survey*, *ArXiv e-prints* (Sept., 2012) [[arXiv:1209.1043](#)].
- [126] S. Joudaki, K. N. Abazajian, and M. Kaplinghat, *Are Light Sterile Neutrinos Preferred or Disfavored by Cosmology?*, *ArXiv e-prints* (Aug., 2012) [[arXiv:1208.4354](#)].
- [127] J. Sollerman, E. Mörtzell, T. M. Davis, M. Blomqvist, B. Bassett, A. C. Becker, D. Cinabro, A. V. Filippenko, R. J. Foley, J. Frieman, P. Garnavich, H. Lampeitl, J. Marriner, R. Miquel, R. C. Nichol, M. W. Richmond, M. Sako, D. P. Schneider, M. Smith, J. T. Vanderplas, and J. C. Wheeler, *First-Year Sloan Digital Sky Survey-II (SDSS-II) Supernova Results: Constraints on Nonstandard Cosmological Models*, *Astrophys. J.* **703** (Oct., 2009) 1374–1385, [[arXiv:0908.4276](#)].
- [128] J. C. Bueno Sanchez, S. Nesseris, and L. Perivolaropoulos, *Comparison of recent S_NIa datasets*, *J. Cosmol. Astropart. Phys.* **11** (Nov., 2009) 29, [[arXiv:0908.2636](#)].
- [129] C. Carbone, L. Verde, Y. Wang, and A. Cimatti, *Neutrino constraints from future nearly all-sky spectroscopic galaxy surveys*, *J. Cosmol. Astropart. Phys.* **3** (Mar., 2011) 30, [[arXiv:1012.2868](#)].
- [130] A. Slosar, *Detecting neutrino mass difference with cosmology*, *Phys. Rev. D* **73** (June, 2006) 123501, [[astro-ph/](#)].
- [131] F. de Bernardis, T. D. Kitching, A. Heavens, and A. Melchiorri, *Determining the neutrino mass hierarchy with cosmology*, *Phys. Rev. D* **80** (Dec., 2009) 123509, [[arXiv:0907.1917](#)].
- [132] R. Jimenez, T. Kitching, C. Peña-Garay, and L. Verde, *Can we measure the neutrino mass hierarchy in the sky?*, *J. Cosmol. Astropart. Phys.* **5** (May, 2010) 35, [[arXiv:1003.5918](#)].
- [133] A. C. Hall and A. Challinor, *Probing the neutrino mass hierarchy with cosmic microwave background weak lensing*, Mon. Not. R. Astron. Soc. (Aug., 2012) 3504, [[arXiv:1205.6172](#)].
- [134] C. Wagner, L. Verde, and R. Jimenez, *Effects of the Neutrino Mass Splitting on the Nonlinear Matter Power Spectrum*, *Astrophys. J.* **752** (June, 2012) L31, [[arXiv:1203.5342](#)].

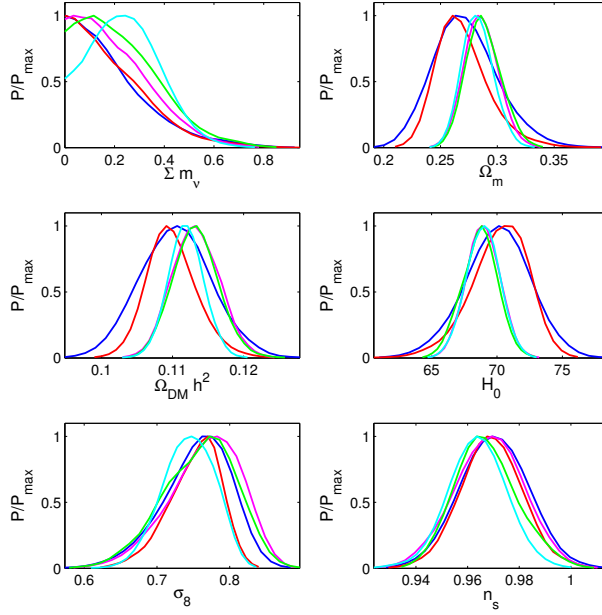


Figure 1. One-dimensional marginalized constraints on individual cosmological parameters from five combinations of different observations, i.e. CMB (blue), CMB+WL (red), CMB+BAO+OHD (magenta), CMB+BAO+SNIa (green), and CMB+WL+BAO+OHD+SNIa (cyan). Here $\sum m_\nu$ is free whereas N_{eff} and w are fixed to their standard values ($N_{\text{eff}} = 3.046$, $w = -1$).

Table 1. Key parameters and their prior information.

Set	Parameter	Symbol	Prior
Vanilla	Physical baryon density	$\Omega_b h^2$	[0.005, 0.1]
	Physical dark matter density	$\Omega_{\text{DM}} h^2$	[0.01, 0.99]
	$100 \times$ Angular size of sound horizon	$100 \times \theta_A$	[0.5, 10]
	Reionization optical depth	τ	[0.01, 0.8]
	Scalar spectral index	n_s	[0.5, 1.5]
	Scalar spectral amplitude	$\ln(10^{10} A_s)$	[2.7, 4]
Extended	Sum of neutrino masses	$\sum m_\nu$ [eV]	[0, 10]
	Effective number of neutrinos	N_{eff}	[0, 10]
	Constant dark energy EOS	w	[-2, 0]
Derived	Total matter density	Ω_m	—
	Power spectrum normalization	σ_8	—
	Hubble constant	H_0	—

The ‘‘Vanilla’’ set of parameters is the basic set that is always fed into our MCMC code with uniform prior distribution, as shown within the table. What we are exceedingly interested in is the ‘‘Extended’’ set of parameters, whose flat prior distributions are also given. By fixating some members of this set while varying the rest, it is possible to investigate individually and collectively the constraints they receive from observational data. And meanwhile we are able to learn some knowledge about how parameter degeneracies affect the constraints. As shown in this table, Ω_m , σ_8 and H_0 are always derived. Additionally, a flat prior ([0, 2]) is assigned to A_{SZ} , i.e. the SZ template amplitude, which is always marginalized as a nuisance parameter.

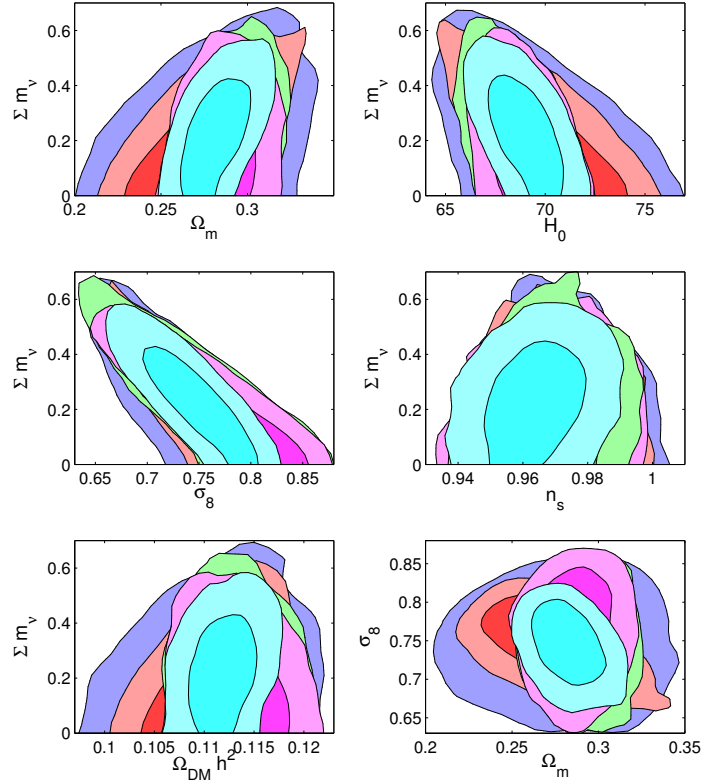


Figure 2. Two-dimensional confidence contours of several parameter pairs from five combinations of different observations, i.e. CMB (blue), CMB+WL (red), CMB+BAO+OHD (magenta), CMB+BAO+SNiA (green), and CMB+WL+BAO+OHD+SNiA (cyan). For each data combination, the inner and outer contours refer to the borders of 68% and 95% confidence regions, respectively. As in Fig. 1, Σm_ν is free here, but N_{eff} and w are fixed.

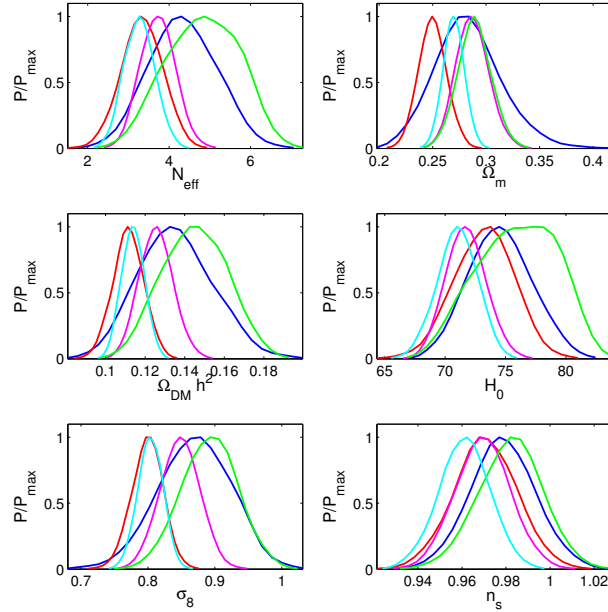


Figure 3. Same as Fig. 1, except that N_{eff} is a free parameter here, with massless neutrinos and $w = -1$.

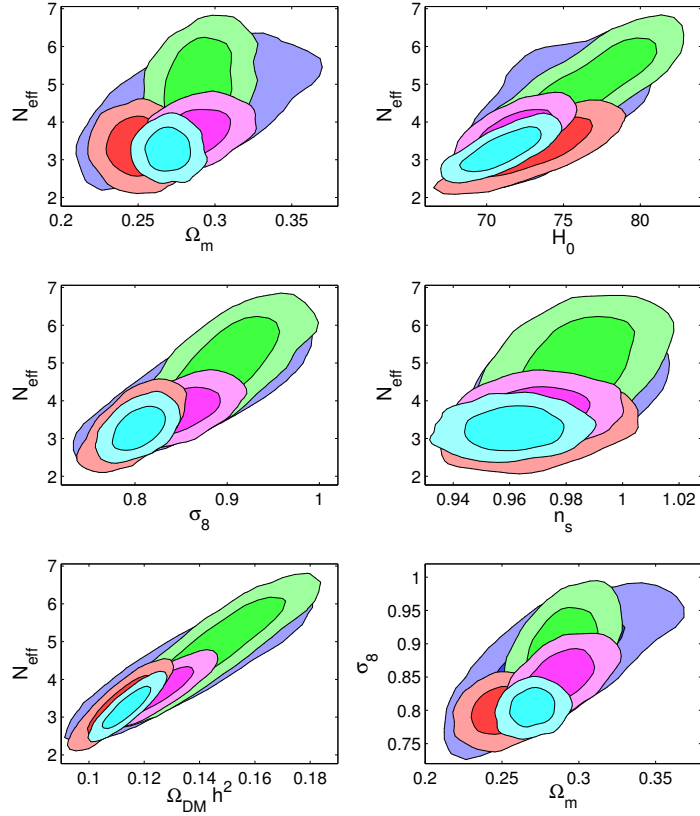


Figure 4. Same as Fig. 2, except that N_{eff} is a free parameter here, with massless neutrinos and $w = -1$.

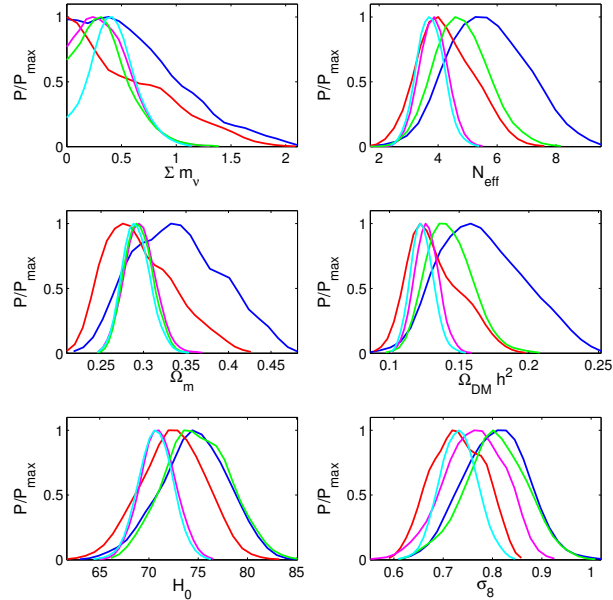


Figure 5. Same as Fig. 1, but for both Σm_ν and N_{eff} kept free, with $w = -1$.

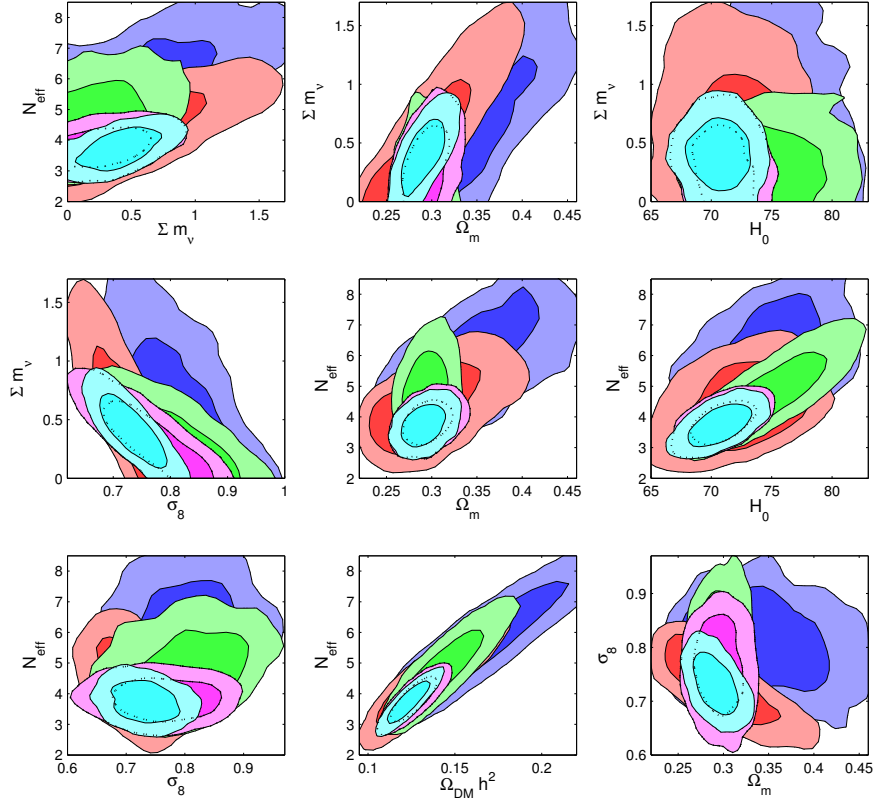


Figure 6. Same as Fig. 2, but for both Σm_ν and N_{eff} kept free, with $w = -1$. For the sake of clarity, the dotted lines in each panel denote the same confidence regions for CMB+BAO+OHD, as shown by the magenta contours.

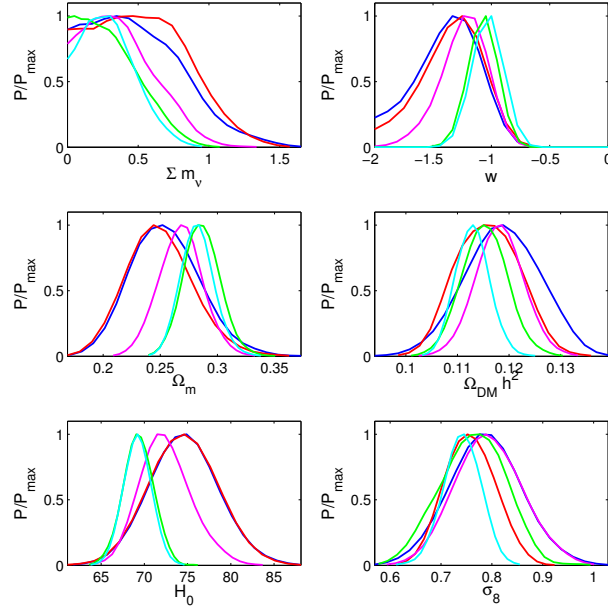


Figure 7. Same as Fig. 1, but also with w freed, and N_{eff} is still fixed.

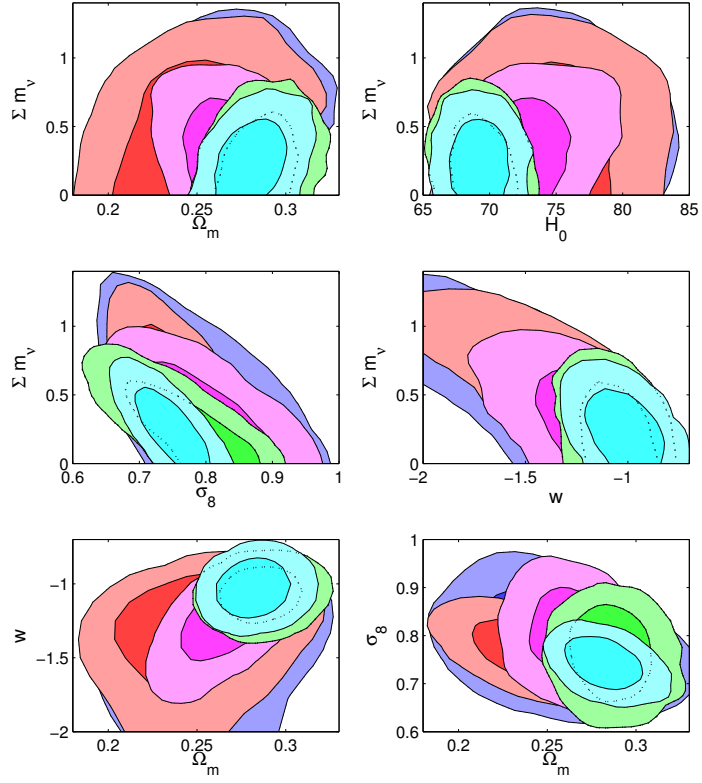


Figure 8. Same as Fig. 2, but also with w freed, and N_{eff} is still fixed. For the sake of clarity, the dotted lines in each panel denote the same confidence regions for CMB+BAO+SNIa, as shown by the green contours.

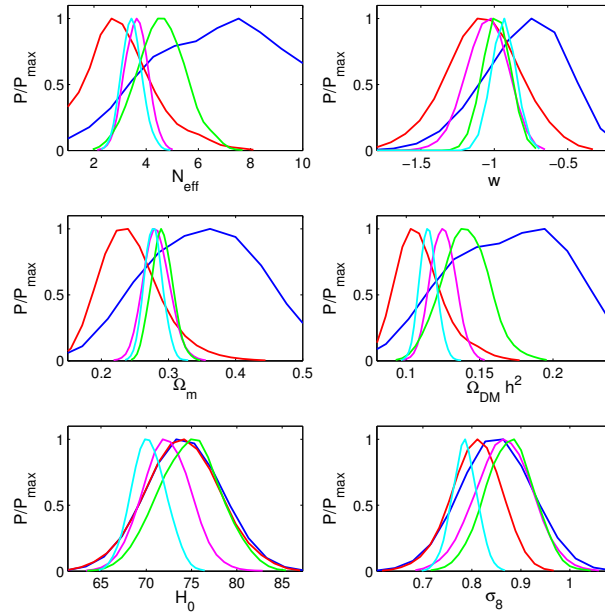


Figure 9. Same as Fig. 1, but here N_{eff} and w are instead free to vary, with massless neutrinos.

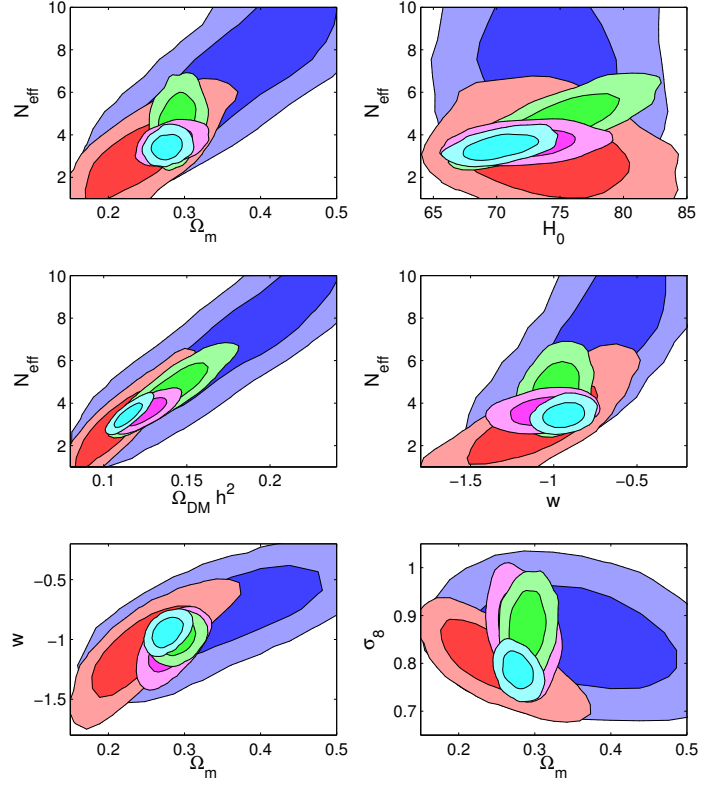


Figure 10. Same as Fig. 2, but here N_{eff} and w are instead free to vary, with massless neutrinos.

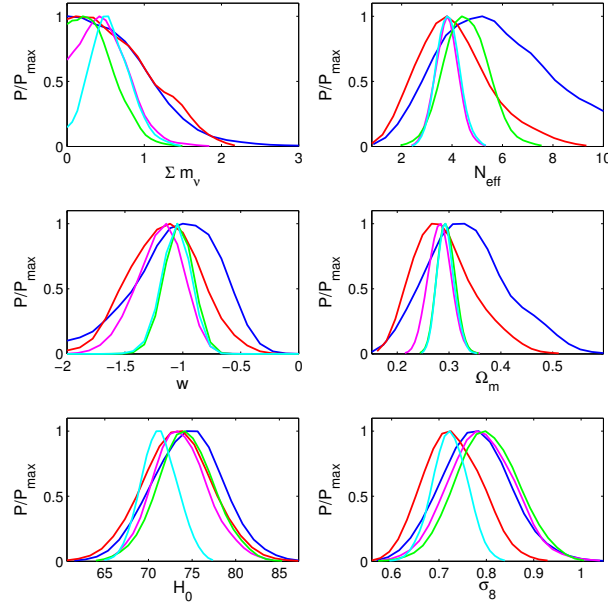


Figure 11. Same as Fig. 1, yet all members of the extended set (Σm_ν , N_{eff} , w) are treated as free parameters.

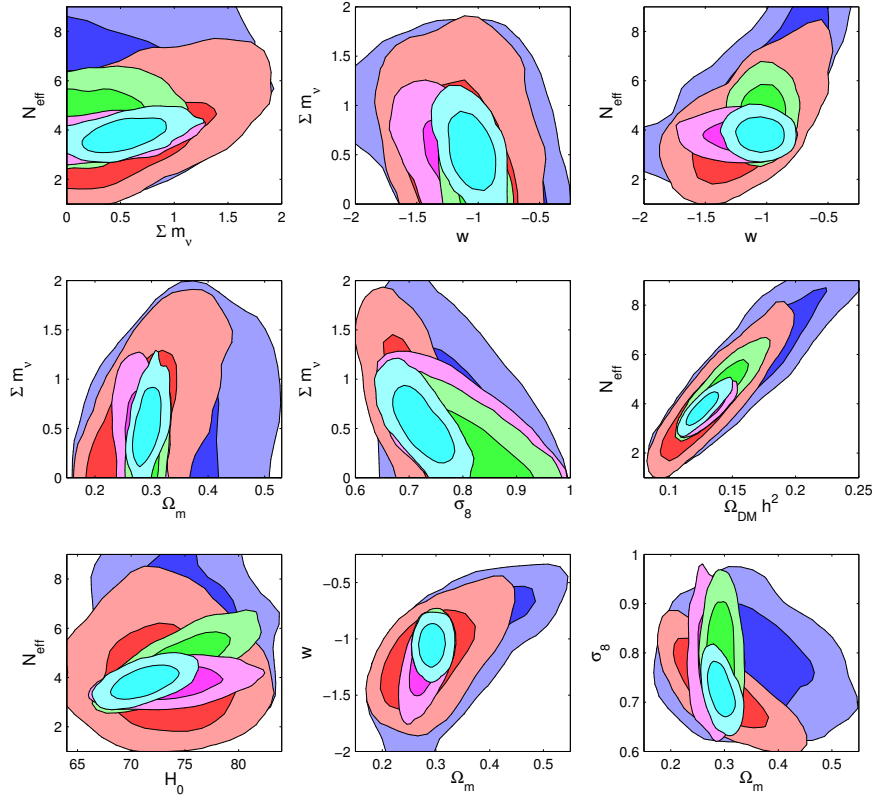


Figure 12. Same as Fig. 2, yet all members of the extended set $(\Sigma m_\nu, N_{\text{eff}}, w)$ are treated as free parameters.

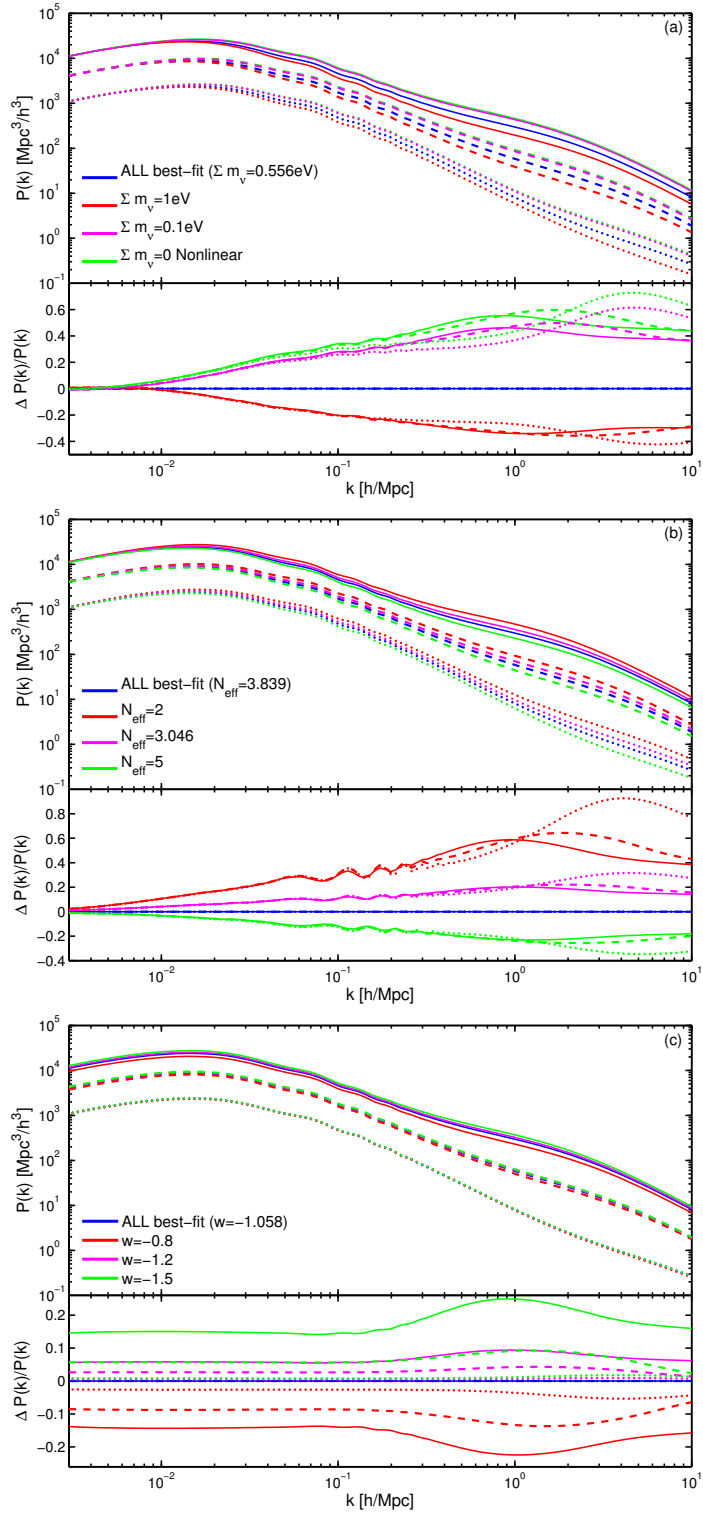


Figure 13. Matter power spectra and their fractional differences. In each panel, the sets of solid, dashed and dotted lines represent power spectra at redshift $z = 0, 1, 3$, respectively. The blue curves in each panel are calculated from the best-fit parameter values when all cosmological probes are considered, with all three extended parameters (Σm_ν , N_{eff} , w) kept free (see Table 7). Compared with the blue set of lines, other sets are computed with only one given parameter altered to the values shown within each panel.

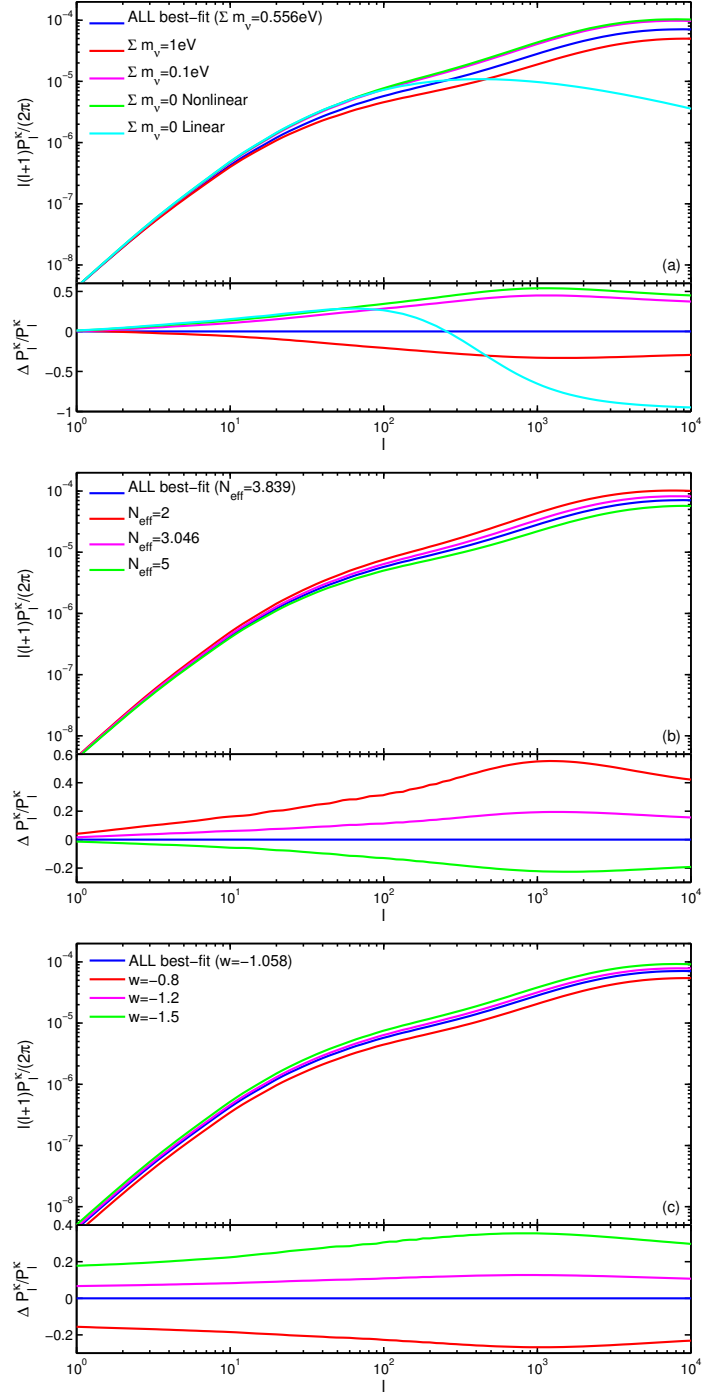


Figure 14. Convergence power spectra and their fractional differences. As in Fig. 13, the blue curve corresponds to the best-fit parameter values given all cosmological data with all of $(\Sigma m_\nu, N_{\text{eff}}, w)$ free (see Table 7). Other lines are plotted with only one given parameter changing its value in order to show the effects of the three extended parameters.

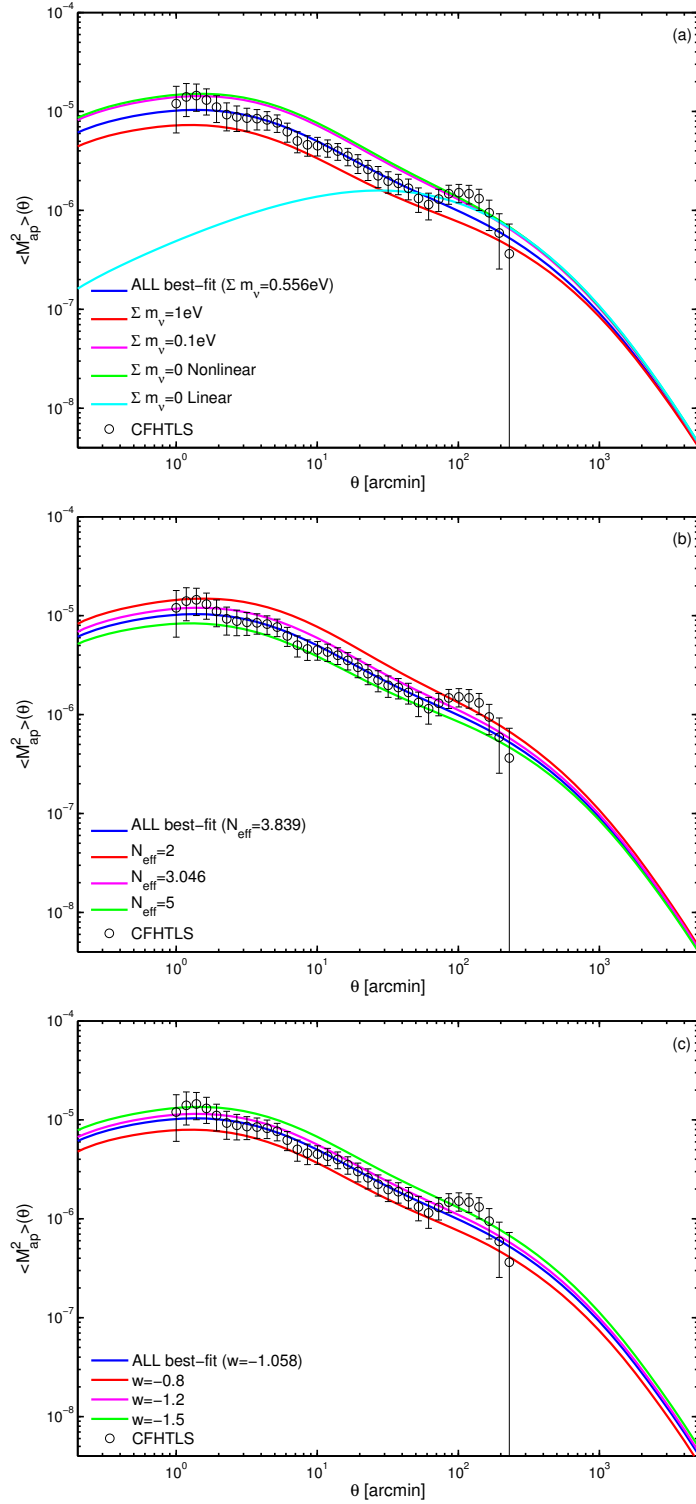


Figure 15. Aperture-mass variance from observation (CFHTLS) and from theoretical calculations. As in Fig. 13, the blue curve is given by the best-fit parameter values against the full combination with all of $(\Sigma m_\nu, N_{\text{eff}}, w)$ free (see Table 7). Other lines are drawn with only one given parameter altered.

Table 2. Constraints on Parameter Scenario of “Vanilla+ $\sum m_\nu$ ” Using Multiple Combinations of Cosmological Probes.

		CMB	CMB+WL	CMB+BAO+OHD	CMB+BAO+SNIa	CMB+WL+BAO+OHD+SNIa
Vanilla	$100\Omega_b h^2$	2.242 ± 0.055	2.241 ± 0.051	2.242 ± 0.051	2.236 ± 0.052	2.229 ± 0.050
	$100\Omega_{\text{DM}} h^2$	11.04 ± 0.49	11.00 ± 0.35	11.33 ± 0.32	11.33 ± 0.31	11.19 ± 0.24
	$10^4 \theta_A$	103.91 ± 0.25	103.90 ± 0.25	103.94 ± 0.25	103.91 ± 0.26	103.88 ± 0.23
	τ	0.090 ± 0.015	0.089 ± 0.015	0.088 ± 0.014	0.087 ± 0.015	0.087 ± 0.014
	n_s	0.970 ± 0.013	0.969 ± 0.013	0.968 ± 0.013	0.967 ± 0.012	0.964 ± 0.011
	$\ln(10^{10} A_s)$	3.073 ± 0.036	3.070 ± 0.031	3.081 ± 0.034	3.076 ± 0.035	3.068 ± 0.030
Extended	$\sum m_\nu$ [eV]	< 0.524	< 0.496	< 0.486	< 0.518	< 0.476
Derived	Ω_m	0.272 ± 0.028	0.270 ± 0.023	0.286 ± 0.015	0.288 ± 0.015	0.283 ± 0.013
	σ_8	0.755 ± 0.046	0.751 ± 0.035	0.766 ± 0.048	0.758 ± 0.049	0.743 ± 0.035
	$H_0/100$	0.700 ± 0.024	0.702 ± 0.022	0.689 ± 0.012	0.687 ± 0.013	0.689 ± 0.012

Concerning the reported results of all parameters except $\sum m_\nu$, the best-fit values refer to the means calculated from one-dimensional marginalized posterior probability distributions, as plotted in Fig. 1 for some parameters. The reported errors originate from the symmetric 68% confidence intervals with respect to the corresponding means. For $\sum m_\nu$, the 95% upper limit is given. Here N_{eff} and w are fixed to their standard values ($N_{\text{eff}} = 3.046$, $w = -1$).

Table 3. Constraints on Parameter Scenario of “Vanilla+ N_{eff} ” Using Multiple Combinations of Cosmological Probes.

		CMB	CMB+WL	CMB+BAO+OHD	CMB+BAO+SNIa	CMB+WL+BAO+OHD+SNIa
Vanilla	$100\Omega_b h^2$	2.215 ± 0.057	2.228 ± 0.057	2.214 ± 0.054	2.213 ± 0.052	2.204 ± 0.052
	$100\Omega_{\text{DM}} h^2$	13.54 ± 1.85	11.15 ± 0.76	12.56 ± 0.83	14.50 ± 1.50	11.39 ± 0.57
	$10^4 \theta_A$	103.42 ± 0.38	103.74 ± 0.37	103.57 ± 0.32	103.30 ± 0.35	103.64 ± 0.33
	τ	0.086 ± 0.015	0.089 ± 0.015	0.084 ± 0.014	0.084 ± 0.014	0.081 ± 0.013
	n_s	0.978 ± 0.014	0.971 ± 0.014	0.969 ± 0.012	0.982 ± 0.014	0.961 ± 0.011
	$\ln(10^{10} A_s)$	3.126 ± 0.048	3.074 ± 0.032	3.105 ± 0.035	3.139 ± 0.040	3.064 ± 0.029
Extended	N_{eff}	4.340 ± 0.817	3.334 ± 0.496	3.722 ± 0.418	4.827 ± 0.843	3.271 ± 0.367
Derived	Ω_m	0.283 ± 0.031	0.250 ± 0.013	0.287 ± 0.015	0.289 ± 0.015	0.270 ± 0.009
	σ_8	0.870 ± 0.053	0.799 ± 0.023	0.848 ± 0.029	0.892 ± 0.041	0.804 ± 0.018
	$H_0/100$	0.746 ± 0.026	0.732 ± 0.024	0.717 ± 0.016	0.760 ± 0.032	0.710 ± 0.016

Same as Table 2, except that N_{eff} is free to vary, with massless neutrinos and $w = -1$. We present the results of N_{eff} following the usual convention as introduced in Table 2.

Table 4. Constraints on Parameter Scenario of “Vanilla+ $\sum m_\nu+N_{\text{eff}}$ ” Using Multiple Combinations of Cosmological Probes.

		CMB	CMB+WL	CMB+BAO+OHD	CMB+BAO+SNIa	CMB+WL+BAO+OHD+SNIa
Vanilla	$100\Omega_b h^2$	2.186 ± 0.058	2.204 ± 0.059	2.214 ± 0.055	2.212 ± 0.054	2.213 ± 0.055
	$100\Omega_{\text{DM}} h^2$	16.75 ± 2.95	13.32 ± 1.89	12.68 ± 0.86	14.35 ± 1.42	12.34 ± 0.80
	$10^4 \theta_A$	103.11 ± 0.34	103.43 ± 0.36	103.56 ± 0.32	103.35 ± 0.35	103.58 ± 0.32
	τ	0.084 ± 0.014	0.086 ± 0.014	0.088 ± 0.015	0.087 ± 0.014	0.087 ± 0.014
	n_s	0.985 ± 0.014	0.976 ± 0.014	0.974 ± 0.013	0.987 ± 0.015	0.972 ± 0.012
	$\ln(10^{10} A_s)$	3.157 ± 0.050	3.097 ± 0.038	3.101 ± 0.037	3.132 ± 0.041	3.086 ± 0.033
Extended	$\sum m_\nu$ [eV]	< 1.515	< 1.393	< 0.758	< 0.775	$0.421^{+0.186}_{-0.219}$
	N_{eff}	5.729 ± 1.274	4.308 ± 0.924	3.843 ± 0.439	4.814 ± 0.889	3.740 ± 0.446
Derived	Ω_m	0.341 ± 0.051	0.297 ± 0.040	0.296 ± 0.018	0.294 ± 0.015	0.292 ± 0.016
	σ_8	0.806 ± 0.063	0.729 ± 0.051	0.762 ± 0.059	0.807 ± 0.063	0.731 ± 0.037
	$H_0/100$	0.746 ± 0.034	0.724 ± 0.032	0.709 ± 0.017	0.749 ± 0.031	0.707 ± 0.017

Same as Table 2, but for both $\sum m_\nu$ and N_{eff} kept free, with $w = -1$. The conventions for presenting the results of $\sum m_\nu$ and N_{eff} are as usual. Only for the full data combination (CMB+WL+BAO+OHD+SNIa), the result of $\sum m_\nu$ is represented by the best-fit value with asymmetric errors marking the ranges of 68% confidence interval.

Table 5. Constraints on Parameter Scenario of “Vanilla+ $w+\sum m_\nu$ ” Using Multiple Combinations of Cosmological Probes.

		CMB	CMB+WL	CMB+BAO+OHD	CMB+BAO+SNIa	CMB+WL+BAO+OHD+SNIa
Vanilla	$100\Omega_b h^2$	2.191 ± 0.059	2.186 ± 0.062	2.214 ± 0.054	2.218 ± 0.052	2.225 ± 0.054
	$100\Omega_{\text{DM}} h^2$	11.87 ± 0.70	11.59 ± 0.57	11.82 ± 0.45	11.53 ± 0.43	11.29 ± 0.31
	$10^4 \theta_A$	103.79 ± 0.26	103.74 ± 0.26	103.87 ± 0.25	103.85 ± 0.26	103.88 ± 0.24
	τ	0.085 ± 0.014	0.086 ± 0.014	0.085 ± 0.014	0.087 ± 0.015	0.086 ± 0.014
	n_s	0.955 ± 0.015	0.954 ± 0.015	0.959 ± 0.013	0.962 ± 0.013	0.964 ± 0.012
	$\ln(10^{10} A_s)$	3.075 ± 0.034	3.063 ± 0.030	3.081 ± 0.034	3.077 ± 0.036	3.067 ± 0.031
Extended	$\sum m_\nu$ [eV]	< 1.079	< 1.072	< 0.819	< 0.688	< 0.627
	w	-1.379 ± 0.247	-1.340 ± 0.237	-1.240 ± 0.182	-1.074 ± 0.088	-1.034 ± 0.080
Derived	Ω_m	0.255 ± 0.029	0.250 ± 0.028	0.268 ± 0.018	0.286 ± 0.016	0.283 ± 0.014
	σ_8	0.788 ± 0.068	0.757 ± 0.047	0.794 ± 0.065	0.762 ± 0.062	0.741 ± 0.035
	$H_0/100$	0.746 ± 0.038	0.746 ± 0.038	0.725 ± 0.029	0.693 ± 0.017	0.692 ± 0.016

Same as Table 2, but also with w freed, and N_{eff} is still fixed. The results of w is presented in the conventional manner.

Table 6. Constraints on Parameter Scenario of “Vanilla+ $w+N_{\text{eff}}$ ” Using Multiple Combinations of Cosmological Probes.

		CMB	CMB+WL	CMB+BAO+OHD	CMB+BAO+SNIa	CMB+WL+BAO+OHD+SNIa
Vanilla	$100\Omega_b h^2$	2.227 ± 0.061	2.230 ± 0.061	2.207 ± 0.053	2.215 ± 0.054	2.212 ± 0.054
	$100\Omega_{\text{DM}} h^2$	17.09 ± 3.72	11.02 ± 1.61	12.52 ± 0.84	14.05 ± 1.56	11.50 ± 0.57
	$10^4 \theta_A$	103.16 ± 0.43	103.82 ± 0.49	103.60 ± 0.32	103.36 ± 0.35	103.60 ± 0.32
	τ	0.086 ± 0.015	0.087 ± 0.015	0.084 ± 0.014	0.085 ± 0.014	0.084 ± 0.014
	n_s	1.002 ± 0.028	0.965 ± 0.026	0.967 ± 0.014	0.980 ± 0.016	0.967 ± 0.013
	$\ln(10^{10} A_s)$	3.173 ± 0.060	3.062 ± 0.047	3.107 ± 0.036	3.133 ± 0.042	3.071 ± 0.030
Extended	N_{eff}	> 2.885	3.192 ± 1.214	3.623 ± 0.432	4.608 ± 0.860	3.454 ± 0.386
	w	-0.794 ± 0.240	-1.076 ± 0.233	-1.054 ± 0.130	-0.986 ± 0.077	-0.937 ± 0.060
Derived	Ω_m	0.354 ± 0.078	0.245 ± 0.044	0.282 ± 0.019	0.291 ± 0.016	0.278 ± 0.013
	σ_8	0.849 ± 0.066	0.807 ± 0.050	0.865 ± 0.056	0.876 ± 0.048	0.785 ± 0.025
	$H_0/100$	0.742 ± 0.037	0.740 ± 0.037	0.723 ± 0.026	0.748 ± 0.033	0.703 ± 0.018

Same as Table 2, but here N_{eff} and w are instead set free, with massless neutrinos. As illustrated in Fig. 9, the upper limit of N_{eff} for CMB is severely affected by the preempted prior ($N_{\text{eff}} < 10$), therefore not trustable. Thus we present its 95% lower limit instead.

Table 7. Constraints on Parameter Scenario of “Vanilla+ $w+\sum m_\nu+N_{\text{eff}}$ ” Using Multiple Combinations of Cosmological Probes.

		CMB	CMB+WL	CMB+BAO+OHD	CMB+BAO+SNIa	CMB+WL+BAO+OHD+SNIa
Vanilla	$100\Omega_b h^2$	2.191 ± 0.062	2.191 ± 0.061	2.197 ± 0.057	2.211 ± 0.055	2.202 ± 0.056
	$100\Omega_{\text{DM}} h^2$	16.40 ± 3.61	13.35 ± 2.40	13.08 ± 0.93	14.07 ± 1.51	12.70 ± 0.86
	$10^4 \theta_A$	103.24 ± 0.45	103.51 ± 0.47	103.53 ± 0.31	103.37 ± 0.36	103.52 ± 0.32
	τ	0.085 ± 0.015	0.084 ± 0.015	0.086 ± 0.014	0.087 ± 0.014	0.086 ± 0.014
	n_s	0.985 ± 0.028	0.967 ± 0.024	0.966 ± 0.014	0.980 ± 0.015	0.970 ± 0.013
	$\ln(10^{10} A_s)$	3.146 ± 0.062	3.088 ± 0.046	3.104 ± 0.036	3.126 ± 0.041	3.089 ± 0.032
Extended	$\sum m_\nu$ [eV]	< 1.606	< 1.539	< 1.035	< 0.869	$0.556^{+0.231}_{-0.288}$
	N_{eff}	> 2.642	4.125 ± 1.426	3.794 ± 0.447	4.574 ± 0.896	3.839 ± 0.452
	w	-1.051 ± 0.335	-1.155 ± 0.278	-1.206 ± 0.183	-1.038 ± 0.088	-1.058 ± 0.088
Derived	Ω_m	0.338 ± 0.075	0.292 ± 0.057	0.282 ± 0.021	0.295 ± 0.016	0.294 ± 0.016
	σ_8	0.779 ± 0.070	0.729 ± 0.058	0.790 ± 0.067	0.802 ± 0.065	0.723 ± 0.036
	$H_0/100$	0.745 ± 0.038	0.733 ± 0.038	0.737 ± 0.031	0.743 ± 0.031	0.712 ± 0.020

Same as Table 2, yet all members of the extended set ($\sum m_\nu$, N_{eff} , w) are treated as free parameters. Likewise, for CMB, the 95% lower limit is given for N_{eff} . Also the result of $\sum m_\nu$ for the full combination is represented by the best-fit along with 68% confidence region. Note that the case where the entire extended set is kept free against the full combination is quoted as “ALL” in Section 4.